ANL-6683

ANL-6683

Argonne National Laboratory

REACTOR DEVELOPMENT PROGRAM

PROGRESS REPORT

January 1963

ANL-6683
Reactor Technology
(TID-4500, 18th Ed.)
AEC Research and
Development Report

ARGONNE NATIONAL LABORATORY
9700 South Cass Avenue
Argonne, Illinois

0530

REACTOR DEVELOPMENT PROGRAM PROGRESS REPORT

January 1963

Albert V. Crewe, Laboratory Director

Division	Director
Chemical Engineering	S . Lawroski
Idaho	M. Novick
Metallurgy	F . G. Foote
Reactor Engineering	B . I . Spinrad
Remote Control	R . C. Goertz

Report coordinated by
R. M. Adams and A. Glassner

Issued February 15, 1963

Operated by The University of Chicago
under
Contract W-31-109-eng-38
with the
U. S. Atomic Energy Commission

FOREWORD

The Reactor Development Program Progress Report, issued monthly, is intended to be a means of reporting those items of significant technical progress which have occurred in both the specific reactor projects and the general engineering research and development programs. The report is organized in a way which, it is hoped, gives the clearest, most logical over-all view of progress. The budget classification is followed only in broad outline, and no attempt is made to report separately on each sub-activity number. Further, since the intent is to report only items of significant progress, not all activities are reported each month. In order to issue this report as soon as possible after the end of the month editorial work must necessarily be limited. Also, since this is an informal progress report, the results and data presented should be understood to be preliminary and subject to change unless otherwise stated.

The issuance of these reports is not intended to constitute publication in any sense of the word. Final results either will be submitted for publication in regular professional journals or will be published in the form of ANL topical reports.

The last six reports issued in this series are:

July 1962	ANL-6597
August 1962	ANL-6610
September 1962	ANL-6619
October 1962	ANL-6635
November 1962	ANL-6658
December 1962	ANL-6672

TABLE OF CONTENTS

TABLE OF CONTENTS

I. BOILING WATER REACTORS

A. BORAX-V

1. Operations and Experiments

a. Reactor Operations. The reactor was operated with the revised boiling core B-2 (see Progress Report for November 1962, ANL-6658, p. 4) at a maximum power of 20.5 Mwt, based on measured feedwater flow, or a power of about 22 Mwt, based on measurement of steam flow, with control rods fully withdrawn. The feedwater flowmeter was recently calibrated against rate of change of water level in the reactor vessel and is considered to be the more reliable measurement. Power was dissipated during the run by venting steam directly to the atmosphere. To minimize the reactivity effect of buildup of fission product poisons, the power approach from 1 Mwt to maximum was made in 2 hr 20 min. At 20.5 Mwt, boiling noise, i.e., variations in the linear flux trace, was ± 2.5% of the power.

The turbogenerator system was operated for 8 hr at 10 Mwt and for 9 hr at 16.5 Mwt. At the end of the 16.5-Mwt run, the control rods were completely withdrawn, and power was being maintained by recirculating 27 gpm of reactor water through heat exchangers and the reactor water demineralizer to the feedwater tank. This procedure led to a slight lowering of the feedwater temperature and core inlet water temperature.

During removal of two fuel rods for checking out gamma-scanning equipment after operation up to 12 Mwt, three chimneys were found to be tipped out of position. Five weighted chimney-positioning clips were designed, fabricated, and installed to lock the chimneys together and restrict movement. Inspection of the chimneys after another week of operation up to the same power showed that this situation has been remedied.

An experiment was performed at reactor powers of 3 and 5 Mwt to determine the effect on reactor performance of partial closure of the atmospheric vent, back-pressure-control steam valve. At 600 psig, starting at a power of 3 Mwt with the steam valve 2% open, the valve was moved to its closed position in about 0.7 sec. (Feedwater measurements prior to the experiment indicated the closed valve was leaking steam equivalent to about 1.7 Mwt. No measurement of valve leakage was made after the test. The system for measuring steam flow was unable to measure this low flow rate accurately.) Power increased to about 3.5 Mwt with an initial period of about 3 sec for about 1 sec, after which the period slowly decreased. The test was terminated after 12 sec at a pressure of 625 psig and power of about 3.8 Mwt by insertion of control rods.

At 5 Mwt, the valve traveled from 13% open to the closed position in 1.6 sec. The power level rose from 5 to 7 Mwt and leveled in 18 sec.

The experiment was terminated by inserting the control rods after 20 sec when the reactor pressure approached the scram pressure.

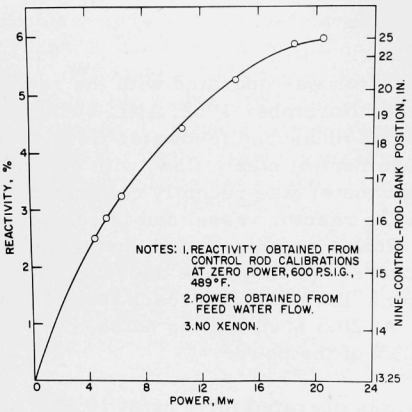

Figure 1. Reactivity vs. Power for the Boiling Core B-2 of BORAX-V

b. Reactor Physics. A curve of reactivity vs. power, plotted from data taken during the maximum power run, is shown in Figure 1. This indicates that, at 600 psig and 489°F, an available excess reactivity of 6% was consumed in going from zero-power conditions to a power of 20.5 Mwt. This yields an average power coefficient of reactivity for core B-2 of about 0.28%/Mwt.

During the periods of operation of the turbogenerator at constant power, measurements were taken to determine the reactivity effect of fission product poisons. These data have not yet been analyzed. Zirconium flux wires were also irradiated at various power levels.

c. Reactor Transfer Functions. BORAX-V transfer functions ($\Delta n/n\Delta k$) were measured with the sine-cosine cross-correlation analog computer at both 10 and 16.5 Mwt. Reactor water temperature and pressure were maintained at 489°F and 600 psig, respectively, throughout each run. The reactor pressure control and the three-element reactor-level control systems were maintained on automatic control for both tests. The 10-Mwt transfer function included data from 0.05 cps to 15.0 cps, whereas the 16.5-Mwt transfer function frequency range was from 0.150 to 15.0 cps. Reproducibility of results was adequate at each frequency studied. In an effort to improve the accuracy of results, between two and six sets of data were run at each frequency. It was found that reproducibility improved with increasing frequency.

In conjunction with the transfer-function analysis, magnetic analog tape and fast-response strip-chart recordings were made with and without the oscillator in operation. Signals recorded on both tape and recorder included fuel temperature (at the center of UO_2 fuel), in-core ion chamber current, out-of-core ion chamber current, and output of sine potentiometer.

The gain of the 10-Mwt transfer function shows a resonance at 1.6 cps with a peak gain of 3.7 db, whereas the 16.5-Mwt transfer function shows a peak gain of 5.2 db at about 2.0 cps (factor of 1.18 increase in gain over 10-Mwt case).

Although the pressure-control system was operated automatically as stated above, it was switched to manual (main-steam-back-pressure control valve held in fixed position, except for slight manual adjustments to regulate reactor pressure) for a comparison of results in the frequency range from 0.1 to 0.6 cps at 16.5 Mwt. Manual pressure control resulted in approximately a 10% greater flux oscillation at the above frequencies. The reason for the greater gain with the fixed valve position is two-fold: (1) manual control caused greater reactor pressure oscillation than did automatic control, because of the omission of the pressure-correcting tendency of the automatic system; and (2) the positive pressure coefficient of reactivity with the attendant greater pressure swings thus caused greater flux oscillations.

d. Root-mean-square Noise-analysis Experiments. The root-mean-square (rms) values of BORAX-V reactor noise were measured at several power levels. Measurements were repeated several times at each power level with resulting good reproducibility. The results are given in Table I. From a plot of the reciprocal of the rms noise current vs. reactor power level, an instability at about 26 Mwt can be predicted.

Table I. Reactor Power vs. RMS Noise Current

Reactor Power (Mwt)	RMS Noise Current (Normalized at 5 Mwt)
5	1.00
10	1.57
14.5	2.15
18.5	3.72
20.5	4.65

e. Water Chemistry. Chemical monitoring of the reactor water during operating periods continued. Water quality, except during the two steam quality tests, was generally satisfactory. The reactor water had a specific resistance equal to or better than 1 megohm-cm during the operating period. The feedwater varied considerably in quality, but its specific resistance remained better than 1 megohm-cm for the entire period, better than 2 megohm-cm for most of the time, and during extended runs ran between 5 and 10 megohm-cm.

Demineralized water in the makeup-water storage tank had a specific resistance better than 3 megohm-cm for most of this period, and is showing a gradual improvement. The leaching out of the Phenoline tank coating is apparently nearing completion. That it has not leached completely as yet is attested by the fact that the water enters the tank at a quality of about 14 megohm-cm and drops immediately to 3 megohm-cm.

Runs during the month have apparently cleaned up the condensate-return system. The condensate initially was returning at a quality of 50,000 ohm-cm. During the extended power runs, it had increased to better than 1.6 megohm-cm. This also indicates that the turbine condenser is not leaking to any great extent.

Both the reactor water and condensate demineralizers performed well at all flow rates. The reactor-water demineralizer consistently produced a water quality of 8.3 megohm-cm, and the condensate demineralizer produced a water quality of 10 megohm-cm or better.

The pH measurements were intermittent, since both sample-station instruments were out of order. The measurements taken, however, indicate that the average pH of the reactor water (excluding the periods for steam-quality test) was 6.7 for the month, with short-period extremes between 5.2 and 8.20.

The chloride concentration remained below 0.1 ppm and generally ran less than 0.05 ppm. The high chloride noted last month during the first operation with condensate returning to the feedwater storage tank was not repeated at any stage of operations this month.

Determinations of the amounts of suspended solids indicate that, in general, a very clean system is being maintained. The concentration of ignited oxides varied from 0.1 to 0.8 ppm. An average of analyses of three samples of the ignited oxides gave the following results in percent by weight: chromium - 1.6%; iron - 38.4%; aluminum - 25.6%; and nickel - 6.9%.

The examination of the surface of the two boiling fuel rods which were removed after operation up to 12 Mwt revealed a hard, adherent, bronze-colored film. Essentially no deposition or corrosion had occurred on the Type 304 stainless steel cladding.

Gas analyses show that the reactor water contains very little radiolytic gas, most of it in the steam. At a power of 10 Mwt, the oxygen concentration in the steam is about 23 cc per liter of condensed steam.

Tests of steam quality by the sodium tracer technique show that at 10 and 16.5 Mwt the steam is very low in moisture (i.e., $< 0.001\%$) in the upper part of the steam dome. The quality profile taken with the movable steam probe shows that in going from a power level of 10 to 16.5 Mwt, the boiling interface is raised approximately 5 in. At 16.5 Mwt, the air-ejector-exhaust system gas before the dilution system was found to be 95% of the lower explosive limit of 4% for H_2. After the dilution system, the explosimeter gave a zero (nonexplosive) reading.

f. In-vessel Instrumentation. Steady-state data at various reactor powers are being accumulated from in-vessel instruments. All thermocouples

except one are now functioning to record various water, fuel, and irradiation-specimen temperatures. The in-vessel pressure transducer has been used to record transient pressures during valve-closing tests. The downcomer drag disk flowmeter and both turbine meters on instrumented fuel assembly I-2 failed electrically before any power operation of the reactor. Failure in the first case appeared to be due to shorted and grounded windings on the "E Core;" in the second case, shorted and grounded coils showed first, and then open-circuited coils.

Maximum fuel temperature recorded at 20.5 Mwt was 1675°F, in fuel rod position 18, core position 46. This fuel assembly has no poison rods and is believed to be in the region of highest reactor flux. The temperature measured was in a fuel rod located 7 in. from the core centerline in the center of the fuel assembly and measured at the core midplane. The effective core radius is 19.5 in.

2. Modification and Maintenance.

Final repair and calibration work was completed on the three-element reactor water-level control and the two reactor back-pressure control valves. Additional delay in valve-stroking time was provided in the two latter valves and the main feedwater control valve (all piston-operated) by relocation of restriction valves and addition of volume chambers to the signal input to the valve positioners. All valves have been adjusted for 10-sec minimum total stroking time. Prior to, and during, the high-power reactor runs, initial settings were made on the three above-mentioned controllers to provide reasonable control action.

A cooling line to the oscillator seal was installed, with provision made for installation of a rotameter. Provision was also made to measure total cooling water flow to the downcomer instrumentation and oscillator. A rotameter has been installed in this line.

3. Procurement and Fabrication

a. The Superheater Core. Since the November Progress Report (ANL-6658, p. 7) the three required central instrumented elements were finished. All central type (standard and instrumented) elements have now been completed. Four more peripheral standard assemblies were welded and with the attachment of transition pieces to subassemblies, the first six peripheral standard elements were finished. All six necessary peripheral instrumented subassemblies were brazed. The first of two peripheral instrumented elements is currently being assembled.

b. Stainless Steel-clad Superheat Fuel. Fifty Type 406 stainless steel-clad superheat fuel plates, containing a dispersion of UO_2 in Type 406 stainless steel, are being fabricated by Atomics International. Inspection

of the plates and assembly of the fuel elements will be done at ANL. These fuel elements will be used in the reactor to test the suitability of Type 406 stainless steel for use under superheater conditions.

It has previously been determined that formation of surface oxide on Type 406 stainless steel has a detrimental effect on the quality of brazed joints. A sodium hydride descaling apparatus has been prepared for removal of scale from the surfaces of the fuel plates to be received from Atomics International. A thin nickel plate will be applied to descaled fuel plate surfaces to prevent reformation of oxide prior to assembly by brazing. Dummy plates are now being descaled and, after brazing, will be evaluated destructively to determine the quality of the braze bond.

II. LIQUID-METAL-COOLED REACTORS

A. General Research and Development

1. ZPR-III, Assembly 42

a. Description. In Assembly 42, a two-zone reactor having a central core area identical with that of Assembly 34, the uranium in the core has an enrichment of 30.7% and an atomic ratio of uranium to carbon of 0.946. The core volume contains only 141 kg of U^{235}, compared with the critical mass of 503 kg in Assembly 34. Assembly 42 was constructed to determine if certain properties of very dilute power reactors could be studied in ZPR-III by building a small, subcritical central area, similar to that of the power reactor of interest, and surrounded by a more highly enriched driver zone, so that the nominally oversized reactor could be fitted into the ZPR-III matrix.

A face view of one-half of Assembly 42 is shown in Figure 2. The central fuel zone (core area) contains one column of enriched uranium, two columns of graphite, two columns of depleted uranium, three columns of stainless steel, and eight columns of reduced-density aluminum per drawer. This central zone is roughly cylindrical and 34 in. in length. The radial periphery of the core zone is surrounded by a $\frac{1}{2}$-in.-thick depleted uranium filter. The driver zone, also 34 in. long, surrounds

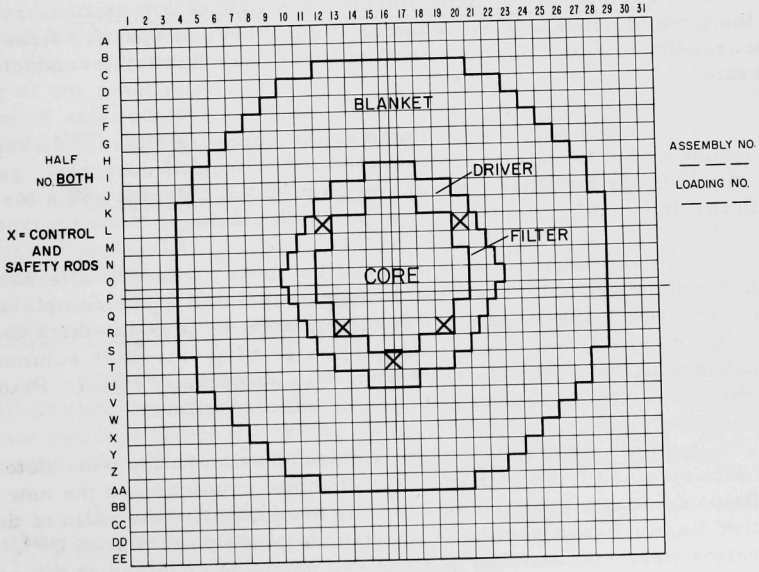

Figure 2. Face View of One-half of Assembly 42, ZPR-III

the radial periphery of the filter. Each drawer in the driver zone contains two columns of enriched uranium, one column of depleted uranium, nine columns of graphite, and four columns of stainless steel.

The core zone contains 141 kg of U^{235}, the driver zone 239 kg, and the depleted uranium filter approximately 0.7 kg. The total critical mass, including the U^{235} in the filter, is slightly over 380 kg of U^{235}.

b. Control Rod Calibration. Control Rod No. 10 was calibrated by measuring periods associated with incremental changes in control-rod position. This control rod, located in the driver region, indicated a worth of approximately 80 Ih, with a differential worth near the center of the rod of approximately 9 Ih/in. The worth of driver material at the edge of the assembly was measured as approximately 25 Ih/kg U^{235}. This worth, along with that from the control-rod calibration, was used to calculate an exact critical mass of 379.4 kg of U^{235} exclusive of the U^{235} in the filter.

c. Plate-orientation Experiments. To check the possibility that core fuel-plate orientation in areas near the filter may have some effect on reactivity, the core fuel plates in four drawers in each half were re-oriented 90° to position these fuel plates parallel to the filter. The results indicated that, within the experimental accuracy of the measurements, there was no change in overall core reactivity.

d. Fuel-bunching Experiments. Because of orientation problems and the limited number of enriched uranium pieces of specific sizes, the heterogeneity experiments for the core and driver had to be conducted separately.

A representative segment of the core was alternately bunched and unbunched. The data, when extrapolated to the full core zone, gave a gain of 193 Ih for bunching from $\frac{1}{8}$- to $\frac{1}{4}$-in.-thick columns and a loss of 122 Ih for unbunching from $\frac{1}{8}$- to $\frac{1}{16}$-in.-thick columns.

A representative segment of the driver was also alternately bunched and unbunched. The data, when extrapolated to the complete driver, indicate a 158-Ih gain for bunching from $\frac{1}{8}$- to $\frac{1}{4}$-in.-thick columns and a loss of 44.6 Ih when unbunching from $\frac{1}{8}$- to $\frac{1}{16}$-in.-thick columns. The unbunching data for the driver zone was abnormally small. Plans are being drawn up to repeat a portion of this experiment.

e. Central Fission Ratios. Central fission ratios were determined from data obtained from both the Kirn absolute counters and the new thin-wall flow counters. The fission ratio, as used here, is the ratio of the effective fission cross section of a particular isotope to that of U^{235}. Fission ratios were measured by placing two opposing counters at the center of the reactor and comparing count rates. In each case, one of the counters

was a U^{235} counter operated as the base counter for the fission ratio and also as a flux monitor to allow normalization from one run to another. Since each counter contained differing amounts of several different isotopes, the fission ratios were calculated from the count-rate data and a set of simultaneous linear equations programmed for the IBM 1620. Only the fission ratios from Kirn counter data have been calculated so far. These fission ratios, along with those measured in Assembly 34 with the Kirn counters, are given in Table II.

Table II. Comparison of Fission Ratios Measured in Assemblies 42 and 34

Ratios	Assembly 42	Assembly 34
$\sigma_{238}/\sigma_{235}$	0.034	0.034
$\sigma_{234}/\sigma_{235}$	0.252	0.247
$\sigma_{233}/\sigma_{235}$	1.426	1.454
$\sigma_{236}/\sigma_{235}$	0.079	0.080
$\sigma_{239}/\sigma_{235}$	1.082	1.067
$\sigma_{240}/\sigma_{235}$	0.282	0.271

f. Fission Traverses. Several drawers along an axial line at the center of the core were modified to accept a $\frac{1}{2}$-in.-diameter thimble. Small counters operated from a traverse mechanism can be positioned remotely at any axial point in this thimble. The relative fission rate as a function of axial position in the core has been measured for U^{235}, U^{238}, Pu^{239}, and U^{234}. The data have not been plotted yet.

g. Nuclear Track Emulsions. Special nuclear track emulsions have been exposed at integrated fluxes of 1×10^8, 5×10^8, and 1×10^9 nvt. They have been sent to Northwestern University for analysis. No data are available at this time.

2. Preparations for ZPR-VI and ZPR-IX Operations

a. ZPR-VI. Additional studies of the leakage rate with the reactor cell pressurized to 10 psig have been initiated. An effort is being made to locate and seal small pin-hole leaks to reduce the leakage rate below the previously obtained value of 6% of the volume per 24 hr at 10 psig.

The fuel-drawer conveyor has been completed by the vendor and will be installed next month.

All parts for the oscillator mechanism to be used in the Doppler effect studies have been fabricated. Assembly and testing of the unit will be the next step in the development.

A changer mechanism for foil counting work is being manufactured by the shops. A shield plate is being fabricated to minimize the radiation exposure to personnel while loading the facility. It will consist of a $1\frac{1}{2}$-in.-thick iron plate placed against (between the two halves) one-half of the matrix.

b. ZPR-IX. Approximately 50% of the aluminum matrix assembly tubes have been reworked and are ready for notching. Bundling of the tubes will start after the notching operation. Production of the aluminum drawers has begun. Installation of coaxial cables between the reactor cell and control console is now in progress. The interlock wiring of the control system has been checked out as far as possible with the single dual-purpose rod drive mechanism on hand. Further checking will wait until receipt of all the dual-purpose drive mechanisms.

B. EBR-I, Mark IV

For the purpose of making measurements of breeding gain, foils were irradiated in thimbles containing simulated fuel elements in selected positions of the core from the center to the core-inner blanket interface. Approximately 150 enriched uranium and 110 plutonium foils were involved in the irradiations, which were accomplished at a reactor power level of one kw.

Measurement of the total beta-gamma activity associated with a completely filled irradiation basket assembly 36 hr after being irradiated resulted in a dose rate of 10 mr/hr at 2 in. Accordingly, loading and unloading operations and subsequent handling will not result in a significant radiation hazard.

Additional irradiations will be accomplished in the inner and outer blankets to provide the necessary destruction and capture information which is required in the breeding-gain calculations.

C. EBR-II

1. Reactor Plant

During the month of January, the major effort in the reactor plant was concentrated on the final operational checkout for fuel handling, which was successfully completed January 25. Miscellaneous minor work in the primary tank and the final cleaning of the tank before closing it up are in progress.

The reactor argon gas system was purged, filled with argon, and put in standby condition for operation when the primary tank is filled with sodium.

The shield and thimble-cooling systems were also operationally checked out on a 24-hr basis for several weeks. The fans and turbocompressors were operated almost continuously during the month, with the refrigeration system being operated intermittently. The systems are essentially ready for sodium filling of the primary tank. The absolute filters were exchanged in the shield and thimble-cooling filter banks under operating conditions without difficulty.

Installation of the argon gas purge control and distribution system for the gas space over the molten seal trough and the new mechanical seal was completed except for installation of gauges and regulators.

Eleven thermocouples, located inside the reactor vessel above the subassembly outlets, were welded to the thermocouple wells (and leak tested) to improve their time response. Other thermocouples in the primary tank were relocated and four additional resistance thermometers were installed.

2. Power Plant

The primary effort in the Power Plant during the month was directed toward preparing the plant for the vacuum-bakeout operation in the sodium-boiler plant. The condensate and feedwater systems were checked out as far as possible. The performance of the motor-driven condensate pump was tested, and the pump-performance curve, as supplied by the manufacturer, was confirmed. Checkout of the startup feedwater pump and, particularly, of the gear motor was accomplished by running the unit uncoupled for a complete shift. Performance appeared to be satisfactory.

Other work, completed during the month, included separating heater drains from turbine drains at the condenser. This should eliminate the possibility of an accident due to backflow in the turbine drain. A valuable dividend was gained by this work by replacing threaded piping with socket-welded fittings. This should assure an air-tight system.

During the last week, the steam system in both the power plant and sodium boiler plant was rinsed of the remaining sodium chromate solution and refilled with demineralized water. Heatup of the steam system was then initiated. After some delays due to minor equipment difficulties, the system was heated to a temperature level of 250°F and the water was recirculated through the evaporators and superheaters.

3. Sodium Boiler Plant

The final phases of work in preparing the secondary system for sodium filling were completed. This included adjustment of all pipe hangers, installation of electrical heaters on the cold trap, final checkout of the argon gas system, and purging of the system with argon. The fire protection system (Ansul) spray nozzles in the basement of the boiler wing were relocated as requested by the safety engineer and in accordance with recommendations of the manufacturer of the equipment.

Instrument checkout was completed and special instruments were provided for measurement of sodium flow, including that from the tank cars to the secondary system storage tank. Temporary exploratory level probes were installed in the storage tank to monitor the level during the entire filling operation.

The sampling system for the secondary system was checked out in readiness for the sodium cleanup operations immediately following the filling of the storage tank.

Final briefing sessions for the shift crews were held prior to heating the first tank car.

On January 21, the approach to sodium filling was started with full operating crews on a three-shift, seven-day-week basis. Rust inhibitor (dichromate) was rinsed from the steam system, which was then filled with water and circulation started. The vacuum pumps temporarily connected to the sodium system were started, and the temperature of the sodium system and steam system were simultaneously raised to 250°F. A vacuum of 90 μ was achieved in the approximately 4000-ft^3 sodium system at the end of the vacuum bakeout. Argon gas was then admitted to the sodium system.

The heating of tank car No. 6 was started on January 28 and continued for approximately 24 hr until the start of transfer of sodium to the secondary storage tank on January 29. The tank car was emptied in 3 hr, and transfer from the second car followed the same time schedule. Some 15,750 gal of sodium have been transferred to the storage tank. The filling operation was accomplished smoothly; only minor difficulties were encountered.

4. Fuel Cycle Facility

Following satisfactory completion of preliminary tests of the Argon Cell pressure-control and cooling system, the cell was purged and filled with nitrogen. Removal of residual oxygen and water vapor from the cell atmosphere was then undertaken by use of the catalytic bed and drying system. Leak-rate measurements were made by determining the increase

in gas inventory and oxygen content. An oxygen level of the order of a few tenths of a percent was reached, but difficulties were experienced with the gas-analysis equipment and with evidence of significant in-leakage of air or inert gas. At present, in-leakage appears to be less than 0.1 ft^3/min. Attempts are being made to isolate or to eliminate possible sources of in-leakage. Removal of oxygen and water vapor continues.

After making minor modifications to the decanning machine to simplify installation, all pneumatically actuated motions of the machine were checked out satisfactorily. Proper operability of the melt-refining furnace vacuum and argon-supply systems was determined, and one furnace was heated to a temperature above 1200°C under vacuum.

Two types of clutches are being tested for use with the drive motors which move the shielding window shutters. These shutters will be used to protect the windows located near high-radiation fields when the windows are not in use. In the absence of a clutch, the shutter drives chatter instead of stalling at the end of shutter travel because of the high stalling torque of the drive motor. Preliminary results indicate the use of a clutch will eliminate the problem of chattering.

The ANL-fabricated fuel-transfer coffin is being shipped out for lead pouring. Some problems still remain in finding a battery-powered system of adequate size for driving the cooling gas-recirculating blower. Conversion to an ac powered system is being considered. The interbuilding coffin now in Idaho has been leak tested and the leaks have been repaired.

5. Fuel Development

a. Fuel-jacket Development for Core II. The Nb-1 w/o Zr tubing (see Progress Report for November 1962, ANL-6658, p. 30) has been sized, finished, delivered, and inspected for irradiation test.

The tubing was delivered in a stress-relieved condition (850°C for 2 hr in vacuum). Later, portions of the tubing were given a full recrystallization anneal at 1400°C for 2 hr in vacuum. The finished tubing was inspected by eddy current and radiographic techniques. Most of the tubing looked exceptionally good and fell well within the 10% maximum allowable defect limit.

Three other niobium alloys, Nb-5 w/o Zr (D-14), Nb-33 w/o Ta-1 w/o Zr (FS-82), and Nb-10 w/o W-10 w/o Ta, are being fabricated into tubing from drilled rod stock. The "tube-blanks" are being drawn to 0.156-in.-I.D. x 0.015-in.-wall tubing. The quantities, while limited, should be sufficient for irradiation test. Each alloy will be delivered in both the stress-relieved and fully recrystallized condition.

b. Penetration Rate of Cladding Materials by Molten Fuels. Safety considerations for EBR-II require information about the rate of penetration of prospective clad materials by molten uranium- and plutonium-containing fuels. Previous work has been done on Type 304 stainless steel and Armco iron with molten uranium and U-5 w/o fissium.[1] An unpredicted decrease in the rate of penetration of iron and stainless steel with increasing temperature was detected. To study this phenomenon further, the penetration rates of Armco iron by molten uranium, U-36 a/o Fe eutectic (melting point 725°C) and U-77 a/o Fe eutectic (melting point 1080°C) as a function of temperature have been determined. A description of the penetration rate variation with temperature of Armco iron in uranium and U-36 a/o Fe was described in the Monthly Report for November, 1962 (ANL-6658, p. 29). A complete tabulation of the data is presented in Table III.

Table III. Penetration of Armco Iron by Molten Uranium, Uranium-36 a/o Iron (725°C Eutectic), and Uranium-77 a/o Iron (1080°C Eutectic)

Clad Material:	Armco Iron											
Fuel:	Uranium				Uranium-36 a/o Iron				Uranium-77 a/o Iron			
Clad Thickness (mils)	15		30		15		30		15		30	
Temp (°C)	Time (sec)	Rate (mils/sec)	Time (sec)	Rate (mils/sec)	Time (sec)	Rate (mils/sec)	Time (sec)	Rate (mils/sec)	Time (sec)	Rate (mils/sec)	Time (sec)	Rate (mils/sec)
740							176,400	0.000169				
850							2,340	0.0128				
950							600	0.05				
1050					84	0.183	216	0.138				
1070							198	0.152				
1085					0.6	25	1.4	21				
1100											199	0.151
1115							0.67	45				
1138			0.9	33								
1150	0.5	30	1.0	30			1.1	27	53	0.278	138	0.217
1169			1.1	27								
1187			1.45	20.5			1.55	19.5				
1206			4.4	6.8								
1229	3.1	4.8	5.7	5.3			3.7	8.1				
1244			5.2	5.8			5.95	5.05			134	0.224
1300			3.7	8.1	1.7	8.8	4.4	6.8	22.7	0.660	53.5	0.561

Armco iron was run against molten U-77 a/o Fe to help understand the high penetration rates found in the 1080°C to 1200°C range in uranium and U-36 a/o Fe. A slow penetration rate was found in the U-36 a/o Fe melt from 740 to 1070°C (this is the range at which UFe_2 forms by the melt reacting with solid iron). The high rate observed from 1080°C to 1200°C is, however, associated with the formation of UFe_2 from two liquids, a high uranium melt and a high iron melt. As was expected, the molten U-77 a/o Fe eutectic alloy did not exhibit a high penetration rate in the 1080°C to 1200°C range because this material does not form UFe_2 compound when put in contact with iron. It is therefore felt that the penetration rate increase is associated with the formation of UFe_2 from the two above-mentioned liquids.

[1] J. Nucl. Mat, 6 281-290 (1962).

c. Properties of Uranium-Plutonium-Fizzium. The properties of U-Pu-Fz alloys (see Progress Report for November 1962, ANL-6658, p. 30) are being studied in order to determine the optimum composition for the Core II loading of EBR-II.

One-inch-long specimens, machined from injection-cast rods, were cycled 100 times between 450 and 700°C for one-hour cycles with holding times of 20 min at 700°C and 15 min at 450°C. The specimens were submerged in NaK which, together with the relatively slow heating and cooling rates, minimized temperature gradients. Specimens of 80 w/o U-10 w/o Pu-10 w/o Fz and 75 w/o U-15 w/o Pu-10 w/o Fz showed very little dimensional changes as the result of thermal cycling. A U-10 w/o Pu alloy, however, lengthened 30%, swelled to a 7% diameter increase, and developed extreme porosity that resulted in a 35% decrease in density.

It is not unusual for uranium alloy castings to develop porosity on cycling between the alpha and beta phases. In this case, extreme general porosity developed with a very large void forming at one end of the specimen. However, it is not clear why a casting should elongate under these cycling conditions. It is possible that a casting grain texture coupled with transformation between the alpha and beta phases on cycling could lead to this.

Specimens of U-10 w/o Pu were machined from $\frac{3}{8}$-in.-diameter injection-cast rods. The tensile strength at room temperature was found to be 35,000 psi, whereas at 502°C it was 19,000 psi. Brittle failure occurred at both temperatures, with elongations being less than 1%.

The brittleness of the U-20 w/o Pu-10 w/o Fs and the U-20 w/o Pu-10 w/o Fz alloys is being studied by impact and hardness testing. In the as-cast condition both alloys have very low shock resistance and hardness values of 30 to 40 R_C. The effect of heat treatment on the brittleness of the U-10 w/o Pu-10 w/o Fz alloy is being determined.

d. Inspection of Additional Core I Jacket Tubing. Type 304 stainless steel tubing is to be used for reloading the EBR-II. It is being tested on a pulsed-differential eddy current test system using a pulse length of 6 μ sec. This month 5776 feet were inspected, bringing the total to date up to 12394 feet.

An electrically conductive, brittle deposit has been found in some of the tubes. Analysis has shown that the deposit contains about the same percentages of iron, nickel, and chromium as does ordinary Type 304 stainless steel, but it is very brittle and very weak, and cannot be tolerated in tubes which will be used for core jackets for a variety of reasons.

Either the ability of the present equipment to detect this condition must be proved, or other test equipment will be constructed and the whole quantity will be retested. In either case, specifications on the maximum area and thickness of deposit will be established before the tubing is retested.

6. Process Development

a. Skull-reclamation Process. The objective of the skull-reclamation process is purification and recovery of fissionable material in melt-refining residues (skull material). The use of partial rather than complete oxidation of the skull material to effect its removal from a melt-refining crucible has been suggested as a method of simplifying the skull-oxidation process and equipment. If partial oxidation of the skull material is the procedure chosen, it may be possible to charge a relatively small amount of oxygen into the melt-refining crucible without using a flowing-oxygen system (which will be needed if complete oxidation of the skull is decided upon). After the skull is partially or completely oxidized, the next step in the Skull Reclamation Process is mixing it into a flux-zinc system for noble metal extraction into the zinc. Since unoxidized uranium as well as the unoxidized noble metals contained in a partially oxidized skull would dissolve in the zinc phase, zinc chloride would be used to oxidize uranium metal into the flux phase.

Earlier runs were successful in showing that skull material can be removed from the crucible satisfactorily after partial oxidation. A run made to investigate the subsequent noble-metal-extraction step showed no difficulty in oxidizing uranium metal with zinc chloride (> 99 percent complete) nor in the subsequent reduction of uranium from the flux phase (about 99 percent complete).

The useful life of a thixotropically cast beryllia crucible (4-in. in O.D., 9 in. high) was 465 hr, the equivalent of 25 precipitation and retorting steps of the skull-reclamation process. This is regarded as very satisfactory performance.

Metal transfers and checkout of the equipment for large-scale (2.5 kg of skull oxide) demonstration of the skull-reclamation process is in progress. Successful separate transfers of flux and metal were made by pressure siphoning. A first attempt to separate metal and flux phases was unsatisfactory. This is attributed to the rapid rate (20 lb/min) used in making the transfer. A rate of transfer of 4 lb/min will be used in the next run. Other operations of the equipment have been highly satisfactory.

As an alternative to using the melt-refining furnace for retorting zinc-and-magnesium-coated uranium from the skull-reclamation process (see Progress Report for December 1962, ANL-6672, p. 19), a distillation crucible, condenser, and collector have been designed and built

which can be used with the melt-refining furnace base. The new design accommodates a larger charge of uranium-zinc-magnesium than was possible in the melt-refining furnace. A test run with the new apparatus had encouraging results. The apparatus was disassembled after the run without sticking, and 97.7 percent of a 50 weight percent magnesium-zinc charge was recovered.

b. Blanket-processing Studies. The blanket process involves dissolution of plutonium-bearing blanket material in a zinc-rich alloy, precipitation of most of the uranium by addition of magnesium, and removal of the plutonium with the remaining uranium in the supernatant phase, which is then boiled down to produce a plutonium concentrate suitable for feeding into the core cycle. The distillation unit to be used in the study of the evaporation of the supernatant product solution has been tested and found to be leak-tight. The power control panel for the unit is being assembled.

c. Plutonium-recovery Process. The distribution behavior of neptunium between liquid zinc-magnesium alloy and molten magnesium chloride at 800°C is being determined. Preliminary results indicate that neptunium exhibits the same general behavior as plutonium (see Progress Report for April 1962, ANL-6565, p. 27).

d. Materials and Equipment Evaluation. Experiments are under way to develop methods for coating or impregnating the surface of a porous, coarse-grained alumina crucible with a solid solution of fused refractory oxides. In one of several attempts, a coating of the eutectic, 41 percent calcium oxide, 52 percent aluminum oxide and 7 percent magnesium oxide, applied as an ethyl alcohol slurry to Norton Alundum crucibles and fired at 1300°C was impermeable to water. Cast alumina crucibles are being coated with slips of the type described above and will be tested for permeability, strength, and resistance to skull oxide extraction and reduction conditions.

e. Removal of Nitrogen from Argon. The removal of nitrogen from the Argon Cell atmosphere in the EBR-II Fuel Cycle Facility is now being considered. Preparations are being made, therefore, to test methods of nitrogen removal on a laboratory scale for the purpose of obtaining data which will aid in the design of plant-scale equipment. Construction of apparatus for the study of the nitridation rate of titanium sponge by nitrogen-argon mixtures in the composition range for 50 to 5000 ppm of nitrogen is nearing completion.

7. Training

Completion of formal classroom systems training for all technicians except reactor operators, of a second 1962 course in Reactor Technology,

of briefing for filling of sodium-systems, and of supplementary training in power generation was achieved by mid-month.

All training is deferred until February to allow adjustment to the routine of shift schedules initiated January 21 and to meet the need for additional manpower in the reactor plant as indicated by the PERT schedule.

D. FARET

A study of the design feasibility, cost, and schedule for the construction of the FARET (Fast Reactor Test Facility) has been initiated to establish a firm base from which to initiate Title I work. The study is being performed by Atomics International, Inc., and an architect-engineer firm, Shaw, Metz and Associates, under the direction and guidance of the Laboratory.

Early results of the study indicate the desirability of locating the reactor vessel within an alpha-gamma cell and the remainder of the primary coolant system within a sealed and shielded vault. The cell and vault provide the necessary biological shielding for the primary system.

The reactor vessel is positioned so that only the vessel cover, which provides access into the vessel, protrudes above the cell floor. An inert gas atmosphere in the cell allows the sodium-filled reactor vessel cover to be removed to permit fuel handling and also to permit some visual observation of the fuel in the vessel during reactor operation. A temporary, transparent vessel cover with suitably sealed openings for insertion of fuel assemblies, equipment, etc., is provided in order that the cell atmosphere can be changed to air and permit the entry of personnel into the cell for the installation of special assemblies into the reactor vessel. If the cell becomes sufficiently contaminated that working within it becomes difficult, the in-cell operation can be accomplished with manipulators.

A conventional-type building is used to house the cell and vault. The building provides an envelope for the controlled release of activity inadvertently released within the building. The building pressure is maintained less than atmospheric to assure that air leakage is into the building during normal usage. The discharge of the building ventilating blowers is passed through filters, and all suspect air is discharged to a stack.

An architect-engineer selection board has been established. Work has been initiated by the board, invitation documents have been drafted, and a project prospectus has been assembled.

III. GENERAL REACTOR TECHNOLOGY

A. Applied Reactor Physics

1. Inelastic Scattering

Some of the results of work performed to date on the inelastic scattering of fast neutrons from niobium, zirconium, and copper is summarized as follows. Measurements were made at 50-kev intervals from the inelastic thresholds to a maximum incident neutron energy of 1.5 Mev, with an incident neutron-energy spread of 20-30 kev. Nanosecond time-of-flight spectroscopy was employed to resolve clearly the individual groups of inelastic neutrons. The differential cross sections for inelastic scattering to residual nuclear levels in copper at 670, 770, 960, and 1114 kev, in zirconium at 920 kev, and in niobium at 740, 810, 960, and 1080 kev were measured. In each instance, the scattered neutrons were emitted isotropically. The normalization of the individual cross sections was determined relative to the known differential elastic-scattering cross section of carbon. The experimental results obtained from the measurement of the gamma rays emitted following inelastic scattering were compared with theoretical calculations based upon Hauser-Feshbach theory.[2,3] Appreciable discrepancies between the various measurements and with the theory are noted. The measured cross sections are summarized in Figures 3-5.

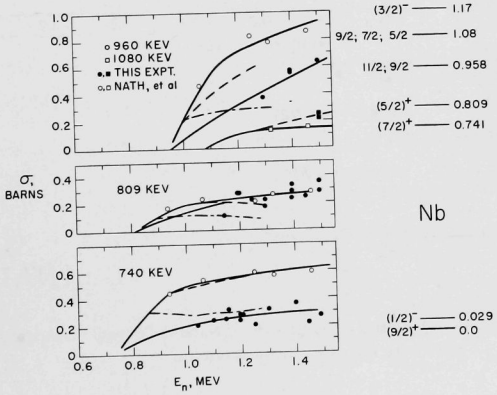

Figure 3. The Inelastic Cross Section of Nb. The solid points refer to this measurement. The open points are from previously reported (n-n'γ) studies. The dotted lines are theoretical predictions.

---

[2]N. Nath et al., Nucl. Phys., 14 (1961).

[3]D. Goldman and C. Luditz, KAPL-2163 (unpublished).

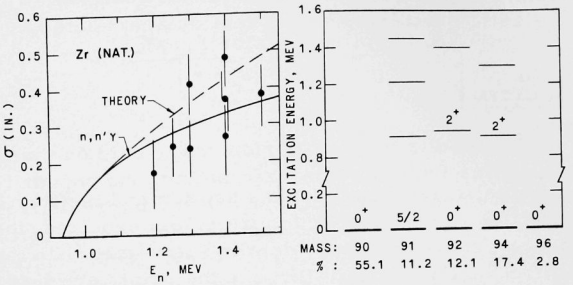

Figure 4. The Inelastic Cross Section of Natural Zr. The solid points are from this experiment. The solid line and dotted line refer, respectively, to (n-n'γ) results and theoretical predictions.

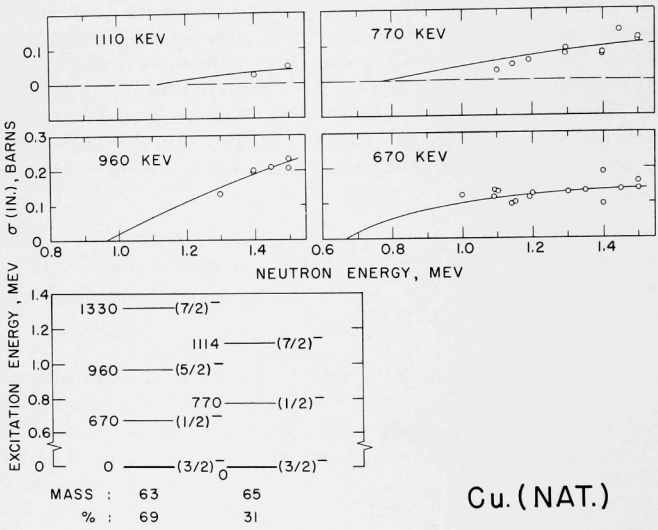

Figure 5. The Inelastic Cross Section of Natural Copper. Experimental results are indicated by open circles.

2. Elastic Scattering of Neutrons from Nickel

The pulse-shape discrimination detector was used to measure the angular distribution of neutrons elastically scattered from natural nickel. Measurements were made with ~ 20-kev neutron-energy resolution in increments of 16 kev from 684 kev to 1235 kev. The data were fully corrected for multiple scattering effects. A least-squares fit to a Legendre

polynomial series was made for each angular distribution. The differential and total elastic scattering cross section are related by

$$\frac{d\sigma(el)}{d\Omega} = \frac{\sigma(el)}{4\pi}\left[1 + \sum_{\ell=1}^{5} W_\ell P_\ell(\cos\theta)\right] .$$

The total elastic-scattering cross section and the five Legendre polynomial coefficients are given in Figure 6. As expected, the polynomial coefficients show much more detailed structure than the total cross section. The smooth curves drawn through the points are just to indicate the structure and do not represent a fit.

3. The $Ni^{58}(n,p)Co^{58m,g}$ Cross Section and Isomer Ratio

The cross sections and isomer ratios for the $Ni^{58}(n,p)Co^{58m,g}$ reaction have been measured relative to the $U^{235}(n,f)$ reaction for neutron energies of 1.04 to 2.67 Mev. The absolute yield of Co^{58} was determined by counting coincidences between the 0.800-Mev gamma ray and the annihilation radiation of the positrons from the decay of the Co^{58} ground state. The observed cross sections and isomer ratios were compared with calculated values obtained by assuming compound-nucleus formation and proton emission only to the 5+ and 2+ states of Co^{58}.

4. Optical Model for Low-energy Neutrons

The results of a study of elastic scattering of low-energy neutrons from spherical nuclei are reported.

The question investigated is how well interactions of low-energy neutrons with undeformed nuclei can be represented by a single, static, local, and spherically symmetric optical-model potential. Calculations have been made for a large range of optical-model parameters by means of the ABACUS-II code. The results have been compared with the following types of available data for nuclei in the mass-number range from 40 to 150: average s- and p-wave absorption (strength functions); total cross sections below 1-Mev neutron energy; scattering cross sections and polarizations by elements consisting mainly of even isotopes and at energies below inelastic thresholds (compound elastic effects were taken into account). The principal difficulty encountered was the apparent conflict between strength-function data (which suggest relatively weak neutron absorption) and scattering data (which suggest much stronger neutron absorption). This difficulty can be resolved by using an imaginary potential that is sharply peaked near the radius of the real potential.

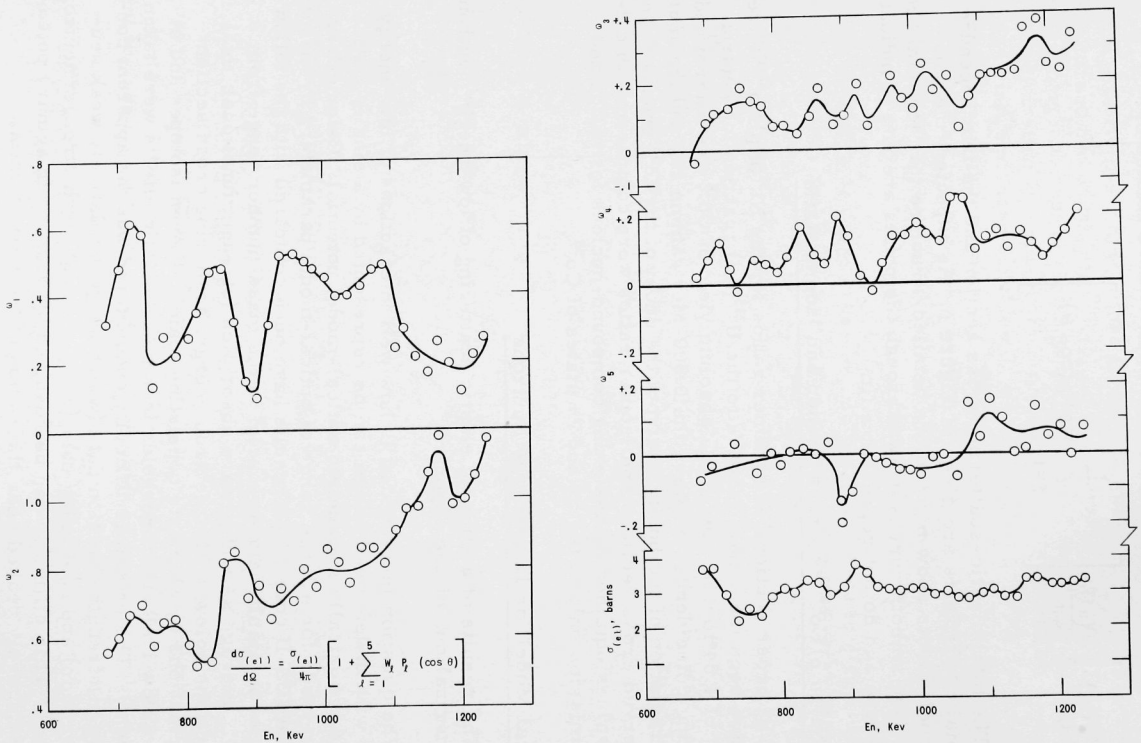

Figure 6. Elastic-scattering Cross Section and the Legendre-Polynomial Coefficients for Nickel

5. High-conversion Critical Experiment - ZPR-VII

In order to correlate the results obtained in the Hi-C program with measurements performed elsewhere on moderately enriched uranium-light-water lattices, an investigation of the properties of less undermoderated lattices was initiated. The critical dimensions and flux patterns have been determined for an assembly of the 3 w/o enriched uranium, stainless steel-clad, Hi-C fuel pins in a 1.24-cm square pitch pattern with every eighth fuel pin removed from the previously assembled uniform lattice. This increased the H/U^{238} atom ratio from 2.9 to 3.9 into a range for which other experimental data exist.

Analysis of the previously obtained data in the uniform lattice experiment (1.24-cm square pitch) is continuing. Foil-activation measurements have yielded approximate values of 1.075 for the fast fission factor and 1.2 for the thermal flux disadvantage factor.

In an attempt to relieve the "bottleneck" in the analysis of foil activation data, the data-reduction program (ANL-807/RE-202) is being modified. The four immediate objectives are to:

(1) increase the reliability of production runs;
(2) increase the usability of the output;
(3) decrease the labor involved in preparing machine input; and
(4) attain operational status as quickly as is reasonably possible.

The importance of achieving the last objective makes it desirable to minimize program changes in accomplishing the first three objectives.

The immediate modifications therefore have been restricted to the following:

(1) make the program compatible with MONITOR operation (OOPS Manual, TM No. 37, AMD);

(2) remove the SENSE SWITCH instructions, thus preventing the machine operator from interfering with the logical flow of the program;

(3) modify the logic involved in the acquisition of weight correction information. In most cases the modified logic permits the weight correction information to be derived from one-tenth of the number of input bits formerly required;

(4) allow for the calculation of either "no weight corrections," "normal weight corrections," or "gold weight corrections;"

(5) automatically list all input data.

These modifications have been made and the program "debugging" completed. A number of other modifications are being made but are not yet operational: accidental coincidence corrections, statistical averaging of multiple counts, and production of punched card output that would serve as input to a curve fitting routine being developed.

6. Recoil Counter for Fast-neutron Spectrometry

Tests which have demonstrated the feasibility of using a hydrogen-recoil proportional counter in a fast critical assembly for spectrum measurements at energies well below 100 kev were reported in ANL-6658 (Progress Report for November 1962, p. 35). Consequently, a probe consisting of a 3.8-cm-diameter proportional counter and preamp is now being constructed for in-pile use in fast critical assemblies. The probe is of minimal mass and will be constructed in a spare stainless fuel box suitable for use in either ZPR-III or ZPR-VI. Reactor time to make spectrum test measurements should be available in the near future.

Concurrently, the problem of correcting the observed pulse distributions for boundary effects is being investigated both experimentally and analytically. A special gridded counter, for guidance in interpretation of recoil spectra which include end and wall effects, has been prepared and tested. The grid structure consists of a fine wire mesh placed very close to the outer cathode of the 7.6-cm-diameter test counter. Grid and cathode are at ground potential. The wire grid shields the cathode and causes a strong field gradient to be established between the grid and ground. The effect of this strong gradient in the wall-effect region is to spread the electron distribution in time, thereby increasing the rise time of events which terminate in the walls. Wall events were recognizable by this means, but the rate-of-rise spectrum was complicated and requires a separate examination of rate-of-rise spectra in coincidence with each ionization interval. Existing electronic systems do not currently have the capability of making the necessary examination, and improvements in circuitry will be required to make the necessary measurements.

Numerical correction procedures required to treat boundary effects in gas-recoil counters are also under consideration. Monte Carlo is the most accurate method, but takes a lot of time and computer analysis. References to iterative procedures done "by hand" (or LGP-30) are also found in older work. The corrections are only reliable for proton recoils of less than a counter radius but are relatively easy to make. A procedure is under investigation which can be applied rapidly with an LGP-30 computer.

7. Absolute Disintegration Rate by Coincidence Counting

Coincidence-counting equipment used for the absolute determination of neutron-absorption rates in manganese baths has been under development. General operational characteristics of both the beta-gamma

(4π-liquid scintillation/sodium iodide) and gamma-gamma (2-liter liquid sample) have now been demonstrated. Over a period of several weeks a satisfactory level of gain stability and reliability have been observed. Checkout and operation of the equipment has been arranged to permit a trained technician to perform a predetermined list of tests (requires 1 to $1\frac{1}{2}$ hr for both systems) in order to evaluate the need for adjustments or note any malfunctions.

Current efforts are directed to eliminating small discrepancies. For example, it was found that great care is required to avoid wall adsorption of radioactive particles in the glass counting vials. The solution to this problem involves a chemical technique: mixing aqueous active solutions with ethanol in a certain optimum proportion before adding to the scintillator. So far, only a few samples having the desired 96% efficiency for Mn^{56} have been obtained; generally, about 93% efficiency is obtained at present.

The persistent problem of after-pulsing in the phototube, which led to extra counts in the beta channel and thereby yielded incorrect disintegration rates, has now been effectively eliminated. The trouble was isolated in satellites from probable positive ion feedback. Although several methods for reducing this effect have been tried, the best compromise is a unique method of paralysis introduction. A 4.5-μsec blocking pulse is placed into anticoincidence with the beta-beta coincidence state of the beta-gamma coincidence system. This effectively introduces a dead time which abolishes the counting of afterpulses from the beta-channel phototubes. No dead-time correction is necessary in coincidence counting, since this same paralysis is presented to both the beta-gamma coincidence analyzer and the beta channel scaler; however, for simple beta counting the count rate loss must be determined.

8. Theoretical Physics

a. Reactor Physics Data Analysis - ZPR-VII. A collision probability program (1692/RE) has been written, in Fortran, which calculates first collision probabilities for either (a) a two-region cylindrical cell, or (b) a two-region slab cell. In the cylindrical case, it is assumed that neutrons incident to the boundary of the unit cell from the inside are returned with an isotropic distribution rather than with the more usual mirror-image reflection, which is unrealistic for small cells. The collision probabilities calculated by the code can be used in calculations of fast fission factors and thermal disadvantage factor calculations for tightly packed lattices. It is planned to use these codes in analyzing data from the Hi-C critical experiments.

b. Doppler-effect Studies. Calculations were made of the s-wave contribution to the capture cross section in U^{238}. No overlap correction

was applied, since it is not expected to be important for U^{238}. The parameters governing the unresolved region above 1 kev are reasonably well known for the s-wave from the measurements for the resolved resonances. For the p-wave, the parameters are not known, and a value of $< \Gamma_n^0 > /D$ was taken so as to give a reasonable fit with the observed capture cross section. Despite the uncertainty in parameters the p-wave contribution to the U^{238} Doppler effect was found to be negligible because of the small change of cross section with temperature.

It has been found previously that the Doppler effect did not appear very sensitive to rod size or to the presence or absence of sodium, provided that in the latter case the low-energy flux had the same normalization for sodium whether it was present or absent. The change in the capture cross section of U^{238}, $\delta\sigma_\gamma$, was found not to be very sensitive to σ_p, the equivalent scattering cross section in barns per U^{238} atom.

Considering that the sign of $\delta\sigma_\gamma/\delta\sigma_p$ changes with energy and that an average over the neutron-energy spectrum takes place, the principal contribution to the U^{238} effect comes in the energy range from 300 to 4000 ev, and little change in effective $\delta\sigma_\gamma$ from one case to another is to be expected. There is a shift in low-energy spectrum shape between the sodium and the non-sodium cases. However, the variation of $\delta\sigma_\gamma$ with energy does not change sufficiently to have an important effect.

It will be of considerable interest to see if the predicted lack of sensitivity of the Doppler effect to the degree of heterogeneity and to the presence or absence of sodium will be verified experimentally.

c. Resonance Integrals. The infinitely dilute resonance integral formulation has been extended to include negative energy levels. The fission and capture resonance integrals were computed for the U^{235} isotope.

The negative-energy single-level parameters used were those reported by Harvey and Sanders[4] and the positive single level parameters are those listed in WCAP-1434.[5] The computed fission and capture cross section at six different energies are given in Table IV. The choice of parameters was checked by comparing the computed fission cross section with the experimental measurements given in BNL-325 Supplement 1. The agreement was found to be very good.

The computed contributions for the resolved positive and negative levels and unresolved levels are listed in Table V. The agreement with experiment indicates that negative levels may make appreciable

---

[4] J. A. Harvey and J. E. Sanders, Progress in Nuclear Energy, Pergamon Press Ltd., Volume 1, p. 6 (1955).

[5] WCAP-1434 (June 1961), Multi-region Reactor Lattice Studies, Appendix V, p. 2.

contributions to resonance integrals and should not be neglected. Similar computations were made for other isotopes having bound levels, and again in many instances the computations were brought into better agreement with experiments. These results will be reported in a forthcoming Reactor Physics Constants Center Newsletter.

Table IV. Computed Fission and Capture Cross Sections of U^{235} at Six Different Energy Levels

Energy (ev)	$\sigma_{fission}$ (b)	$\sigma_{capture}$ (b)
0.025	581.3	118.8
0.108	241.1	46
0.191	189.4	37.91
0.274	202.3	45.05
0.357	130.5	25.53
0.440	100.5	17.96

Table V. Computed Contributions to the Resonance Integrals (RI) for Capture and Fission Cross Sections for Resolved Positive and Negative Energy Levels and the Unresolved Energy Levels

	RI (fission)	RI (capture)
Resolved positive levels	153.9	135.4
Unresolved levels	57.7	43.8
Negative levels	52.8	9.0
Total	264.4	188.2
Experimental[6]	{ 271 274 ± 11	

B. Reactor Fuel Development

1. Ceramic Fuels

a. Irradiation of UO_2 Pellets in Collapsed Aluminum Tubing. The examination of the second of two assemblies, ANL-2-16, consisting of three aluminum-clad UO_2 pellet rods is in progress. Examination of the first irradiated prototype element was described in the Progress Report

[6]Reactor Physics Constants Center Newsletter No. 1.

for April, 1962 (ANL-6565). The cladding alloy is A-288 wrought aluminum. Two rods contained square end pellets and one had pellets with 0.024-in. dished ends. The 0.030-in. cladding on one square pellet rod was precollapsed onto the fuel pellets before irradiation. It is assumed that the cladding of the other rods, assembled with a 0.001-in. helium annulus, collapsed onto the pellets during irradiation in the pressurized water loop in the MTR. The assembly was irradiated to a maximum burnup of 8600 Mwd/T oxide at a maximum $\int \frac{T_0}{T_s} k d\theta$ rating of 50 w/cm.

The dished pellet rod, irradiated in the center of the three-in-line configuration, was bowed both above and below the center brace of the assembly. Measurements of the axial change indicated that this rod had elongated 0.12 in., contrary to the excellent axial stability observed for the dished pellet rod of the first assembly. One square pellet rod elongated 0.020 in. while the other shortened 0.001 in. Diameter measurements on three rods proved to be inconclusive because of heavy scale formation. After descaling, the cladding was excessively pitted, and the surface not amenable to further meaningful measurements of diameter.

The horizontal irradiation of the assembly in the loop produced a virtually linear activity profile from one end of the assembly to the other. This was determined by gamma scanning each rod with a cadmium sulfide photocell which directly fed a millivolt recorder. The activity profile was also evident from the heavier concentration of oxide scale at the hot end of each rod.

The rods were tested for leaks in an immersion bubble-test apparatus. A small hole, about $\frac{3}{32}$ in. in diameter, was found at the base of one weld closure at the cooler end of the dished pellet rod. The other two rods were sound. The intact rods were punctured for fission gas release; aliquots of the released gases are being analyzed by mass spectrometry.

The rods are being sectioned for metallographic examination of the cladding and fuel. The only rod sectioned to date contains a symmetrical central void at the hottest end of the rod. The void is $1\frac{3}{4}$ in. in length, about $\frac{3}{32}$ in. in diameter, and is surrounded by a $\frac{1}{4}$-in.-diameter area of columnar grains. The position and extent of the void corroborates the steep activity gradient from one end of the rod to the other that was found by gamma scanning.

b. Urania with Burnable Poisons. As an introduction to a study of the feasibility of incorporating burnable poison materials in ceramic-type fuels, (see Progress Report for November 1962, ANL-6658, p. 40), a preliminary evaluation of the resistance of sintered urania-rare earth

oxide compositions to high-temperature steam corrosion was carried out. Compositions of 97 w/o UO_2-3 w/o Gd_2O_3, 97 w/o UO_2-3 w/o Dy_2O_3, 97 w/o UO_2-3 w/o Sm_2O_3, and 97 w/o UO_2-3 w/o Eu_2O_3, were compacted at a pressure of 3.36 metric tons per square centimeter and were sintered at 1700°C for 4 hr in a hydrogen atmosphere.

There were no significant changes in the weight, dimensions, or appearance of the sample pellets after exposure to 650°C oxygenated steam at 600 psi pressure for one week. Whereas rare earth oxides are readily subject to attack by moisture, the sintered pellets were not attacked, indicating a reaction between the urania and the rare earth oxide which limited the availability of the oxide for reaction with water. Evaluation of the corrosion resistance of the urania-rare earth oxide compositions is being continued.

Compacts of urania and ceria were pressed at pressures of 1.68, 2.52, 3.36 and 4.20 metric tons/cm^2. The pellets were sintered in an argon atmosphere at temperatures of 1500, 1600, 1700, and 1800°C for 4 hr. Compacts of UO_2 were sintered under the same conditions for purposes of control. Densities for the 100 w/o UO_2 in argon varied from 9.81 gm/cm^3 (1.68 tons pressure, 4 hr at 1500°C) to 10.13 gm/cm^3 (1.68 tons pressure, 4 hr at 1800°C).

The sintered density (9.93 gm/cm^3) of the composition 99.5 w/o UO_2-0.5 w/o CeO_2 was highest for samples pressed at 3.30 metric tons/cm^2 and sintered at 1800°C. The sintered density of 99 w/o UO_2-1 w/o CeO_2, under the same optimum conditions, was also 9.93 gm/cm^3. An increase in ceria to 97 w/o UO_2- 3 w/o CeO_2 decreased the sintered density, under the same conditions, to 9.63 gm/cm^3.

c. Uranium Carbide and Sulfide. An investigation was initiated to determine the equilibrium phases present up to the melting temperatures of composition in the UC-US binary. Materials used to compound the composition were an arc-melted UC ball milled to $< 15\ \mu$ and US made by reacting H_2S with hydrided uranium metal.

Compositions containing 2.5, 10.0, and 20.0 mole percent of US with uranium carbide were compounded, mixed, and formed into small pellets. The specimens were reacted in vacuum for a period of 3 hr. Equilibrium was not obtained, as can be observed from the following data calculated from X-ray diffraction patterns:

	Unit Cell Size, Å	
	UC	US
2.5 m/o US	4.963	no reflections
10.0 m/o US	4.964	5.394
20.0 m/o US	4.968	5.378

Compositions containing 5, 10, and 20 m/o additions of UC were also made and sintered at 1825°C for 3 hr in vacuum. A progressive inhibition of grain growth with increased UC content was readily apparent in the specimen pellets. X-ray diffraction patterns showed only a single cubic phase, indicating complete solid solution. Lattice parameters showed a linear decrease from US to the 20 m/o UC composition, having about a 26% positive deviation from Vegard's law. A further heat treatment will be run at 1825°C to assure equilibrium conditions.

d. Uranium, Thorium, and Plutonium Phosphides. The objective of this study is to characterize the compounds in the various phosphide systems and evaluate their potential as reactor fuel materials. Compounds are currently being synthesized by reaction of the elements, although other methods will be investigated.

All the UP synthesized thus far contained from 1.07 to 1.25 w/o oxygen, corresponding to a UO_2 content of 9.0 to 10.5 w/o. Analysis of fresh uranium metal powder derived from turnings and from plates, both comminuted by hydriding steps, gave oxygen contents of 0.22 w/o and 0.33 w/o, respectively. The remaining oxygen found in the UP could only have come from the phosphorus or the oxygen contamination in the glovebox. Although the uranium powder is stored in a sealed container within the glovebox, the quantity used for preparation of a specimen must be exposed to the glovebox atmosphere for several minutes during preparation of the pellet. The absence of a known technique for determining oxygen content in phosphorus is unfortunate, although the manufacturer claims negligible oxygen contamination in the high-purity material used. Experiments currently under way will hopefully shed light on the sources of the oxygen contamination.

Heating of oxygen-contaminated UP in a vacuum at elevated temperatures may be a feasible purification method. Such material, which initially had an oxygen content of 1.22 w/o, showed an oxygen content of 1.06 w/o after 4 hr at 2000°C. This decrease was further confirmed through analysis of the condensate at the top of a tungsten crucible in which about equal amounts of UP and UO_2 were fired at 2000°C. X-ray diffraction showed the condensate to consist of about 80 w/o UO_2, 10 w/o UP, and 10 w/o U. This method will be evaluated further along with vaporization studies of UP.

Samples prepared across the entire UP-UO_2 compositional range were heated to 2000°C in vacuum. Preliminary X-ray examination shows that the two phases are compatible throughout and that they do not form an intermediate compound. Metallographic and chemical analyses are under way. Melting-point determinations will be conducted to obtain a melting diagram for the system.

Uranium monophosphide is quite resistant to oxidation in air at room temperature. Polished specimens retain this bright metallic sheen after months of exposure to the atmosphere. Moreover, UP is not pyrophoric and can be ground in air with only negligible oxygen pickup. Chemical analysis showed that the oxygen content of UP only increased from 1.22 to 1.29 w/o after 10 min of grinding in air.

Differential thermal analysis studies of UP in a flowing atmosphere of oxygen revealed that its oxidation behavior contrasts markedly with that of UC, UN, US, and UAs. Although the latter four compounds ignite in the temperature range from 300 to 400°C to form U_3O_8, the phosphide exhibits relatively gradual oxidation until 560°C, at which temperature all of the UP has been oxidized. X-ray analysis at this point only reveals UO_2, although the presence of a vitreous substance is indirectly inferred. Another exothermic peak occurs at 650°C, possibly representing oxidation in the vitreous phase, and oxidation of the UO_2 to U_3O_8 finally occurs at 750°C. Small amounts of crystalline UP_2O_7 were detected in material heated to 700°C, and an unknown crystalline phase made its appearance at 800°C, becoming very prominent above 900°C. This phase is believed to be a compound of U_3O_8 and phosphorus pentoxide. Further work is planned to establish the composition of the vitreous phase.

The vitreous coating appears to be responsible for inhibiting oxidation of UP at moderate temperatures and explains the nonpyrophoric and nontarnishing nature of the compound at room temperature. Among the five compounds studied, only UP appears to develop a protective vitreous coating.

Samples of UP containing about 10% of UO_2 were pulverized to pass a 325 mesh screen and pressed into pellets using stearic acid binder. Forming pressures of 20,000 and 40,000 psi were used, and samples were heated in vacuum for $\frac{1}{2}$ hr at 2000°C. The fired pellets were sound and had densities of 87 and 92% of theoretical for those pressed at the lower and higher pressures, respectively. These data are preliminary, since the sintering behavior of UP may be quite different in the pure state.

2. Fabrication of Uranium-Molybdenum Alloys

A program is under way to investigate the fabrication of U-Mo alloys which will contain molybdenum in the range from 3 to 17 w/o. Such alloys will be used for irradiation test specimens to determine their suitability for EBR-II blanket rods should the need arise. Early results have shown that no particular fabrication problems are encountered in the alloys with lower Mo content. However, difficulties become more frequent and the fabrication problems more complex with Mo contents above about 12 w/o.

Investigation of fabrication methods for a U-14 w/o Mo alloy is under way. First attempts at clad rolling were unsuccessful. Further rolling attempts will be made. Multiple casting and extrusion techniques will also be investigated.

3. Corrosion Studies

a. Stainless Steel. A static 80-day test has been completed for Type 304 stainless steel in steam, at 650°C, at 600 psi, that contained 30 ppm oxygen. Defilmed metal weight losses have been used to determine the average corrosion curve. During the first two weeks of test the samples corroded about 0.0005 in. Subsequently, the corrosion rate was approximately linear at about 1 mil/yr. The metal surface was not smooth, and some micropits extended up to 0.003 in. below the average surface.

The dynamic test facility has just completed a five-week test of Types 304 and 406 stainless steel in oxygenated (30 ppm) steam at 650°C and 600 psig. Flow rates of 100, 200, and 300 ft/sec are used simultaneously. To date, only the defilmed data for the first two weeks have been analyzed, but thus far the data obtained with Type 304 stainless steel parallel the static corrosion curve. Also, no effect of flow velocity has been noted for Type 406 stainless steel. The latter shows only about 25% of the metal loss obtained with Type 304 stainless steel.

b. Lightweight Alloy for Use with Mercury. Zirconium nitride has been evaluated as a possible inhibitor in reducing the corrosion of titanium by mercury at 538°C. The tests were initiated on the basis of (1) previous test results with zirconium as an inhibitor, (2) the excellent corrosion resistance of nitrided titanium coatings, and (3) the high solubility of zirconium nitride in mercury at the temperatures of interest. The tests were conducted in quartz capsules containing saturated solutions of additives. Table VI shows the results of 14 days of continuous exposure at 538°C under static conditions.

Table VI. Interaction of Titanium, Zirconium, and Zirconium Nitride Exposed to Liquid Mercury at 538°C

Sample	Test Condition	Weight Change,* mg/cm² (14 days)	Spectrochemical Analysis Exposed Surfaces**	
			Mercury	Zirconium
Crystal bar titanium	Liq Hg	-6.67	W	T
Crystal bar titanium	Liq Hg + Zr	-0.28	M	M
Crystal bar titanium	Liq Hg + Zr Nitride	-2.84	M	M

*Average of two samples

**M - Moderate, 1% to 0.1%; W - Weak, 0.1 to 0.01%, and T - Trace, 0.01 to 0.001%.

It has been shown that zirconium nitride is not as effective an inhibitor as zirconium under identical conditions. The weight loss of titanium samples tested in saturated mercury solutions of zirconium nitride is somewhat lower than that in uninhibited mercury. However, metallographic observation indicates a newly formed compound, possibly nitride, embedded in the matrix of pure titanium. Preferential corrosion occurred at these inclusions. The surface film was not adherent. Spectrochemical analysis revealed uneven mercury distribution on exposed surfaces.

c. Aluminum Powder Products. The French powder products (see Progress Report for November 1962, ANL-6658, p. 40) continue to appear to be in very good condition after an exposure of about four months at 290°C in refreshed water. This exposure has developed extensive blistering and swelling of the cut edges in most of the other powder products tested, so a mild optimism is warranted for these materials.

d. Corrosion of Miscellaneous Materials in Water and Steam. A series of TD nickel samples are now under investigation. This material contains a fine dispersion of thoria to improve high-temperature service properties of the nickel, especially strength and creep resistance. Reportedly, oxidation resistance may also be superior. Samples of "A" nickel are being tested for comparison with DuPont TD material, which contains 2 w/o thoria.

Bar stock samples of each material are being tested in degassed, distilled water at 360°C and in oxygenated steam at 650°C and 600 psi. After short exposures, the TD nickel displayed lower weight gains. However, its surface, especially in steam, was less uniform, developing numerous small blisters visible without magnification. This test is continuing.

In another test, cold-rolled TD nickel is being compared with annealed "A" nickel sheet in oxygenated steam at 650°C and 600 psi. Both etched and merely degreased surfaces are being exposed for each material. No results are available at present.

4. Fuel-jacket Development for High-temperature Applications

As reactor temperatures increase, some of the presently used hardware materials reach operational limits and higher temperature materials are required. Extensive effort has been devoted to the refractory metals W, Mo, Ta, Nb, and their alloys during the past several years, and advancement in general technology has been most encouraging. Some of these materials should meet the challenge and fulfill the requirements. Unfortunately, most of the work has been directed to other than nuclear applications and for finished shapes other than tubing.

Some refractory metal tubing is becoming commercially available for the lower end of the temperature range. For the higher temperatures (up to 2000°C) tubing fabrication becomes more difficult and suitable refractory metal tubing is not available. Accordingly, process development becomes mandatory if hardware technology is to keep pace with the advances in reactor concepts.

The molybdenum base alloy TZM (Mo-0.5 w/o Ti-0.08 w/o Zr-0.02 w/o C) looks promising for such applications. In addition to good high-temperature properties, the Mo-base alloys are much cheaper than most of the other refractory metals. It would seem, therefore, both reasonable and necessary to obtain fabrication knowledge of this and similar materials.

A wrought bar of TZM was machined into $\frac{3}{4}$ in. O.D. x $\frac{1}{4}$ in. I.D. x 1 in. long extrusion blanks for developmental extrusion of tube blanks measuring $\frac{3}{8}$ in. O.D. x $\frac{1}{4}$ in. I.D. x 6 in. long at Super Alloy Forge, Inc. in Hamburg, Michigan. Billets were extruded on a mechanical press at temperatures ranging from 1760°C to about 1925°C. The MoO_3 formed while transporting the heated billet to the press was used as a lubricant. From ten extrusions, five had acceptable surfaces, four were severely cracked and pitted, and one failed to extrude (the first billet). From the work done, it appears that extrusion of tube blanks is feasible. Metallographic examination of a good section of tubing showed good wall uniformity and concentricity. A longitudinal section showed a highly elongated grain structure with no evidence of recrystallization. Sections of acceptable tubing have been annealed for one hour at 1550°C prior to further fabrication into small-diameter, thin-wall tubing.

In addition to TZM, tubular shapes of Mo-0.5 w/o Ti, Mo-30 w/o W and Nb-5 w/o V-5 w/o Mo-1 w/o Zr (B-66) are in various stages of development at ANL. Other refractory metals and alloys, such as Ta-10 w/o W, Ta-8 w/o W-2 w/o Hf, Ta-30 w/o Nb-7.5 w/o V, Nb-10 w/o W-1 w/o Zr-0.1 w/o C (X-110), and W, have been ordered in rod stock form. These materials will be processed into tubing, upon receipt.

5. Nondestructive Testing

a. Ultrasonic Imaging. Life tests on a sealed-off ultrasonic pickup tube having a 2-in. diameter, 2-megacycle quartz target have recently passed the 1000-hr mark. The tube still has good electron emission and has shown no sign of excessive gassing. Parts for several more of these tubes are now in process.

Equipment needed to set up a television ultrasonic imaging system, patterned after the system now in use at Northwestern University, is now being collected.

b. Development of Improved Transducers. Several successful models of operational transducers were fabricated some time ago using a tungsten-loaded epoxy as the backing material. It was noted at this time that a shorter pulse length would be desirable for applications where resolution was a major factor in an ultrasonic test.

With this thought in mind, efforts in the past month were concentrated on improving the transducer backing. One transducer, utilizing fiberglass-loaded epoxy, produces pulses about one-half the length of earlier models. Part of the success in shortening the pulse length was due to the addition of backing material along the edges of the crystal.

One transducer with an external ground through the water was designed and fabricated. This type of ground was obtained by facing the front side of the crystal with silver-loaded epoxy. Preliminary tests, conducted statically, showed it to be comparable with transducers with conventional internal grounds.

Of the many visual methods for studying ultrasonic fields, the Schlieren optical system appears to be the most logical for our purposes. Such a system will be useful in studying transducer patterns and subsequently, the effects of various specimens on ultrasonic beams. Necessary parts for building a Schlieren system will be ordered shortly.

c. Neutron Imaging. Technique curves for neutron radiographic inspection of natural uranium, lead, tungsten, and steel, obtained with the Juggernaut reactor neutron beam, have been completed for thicknesses up to 3 in. The direct-exposure curves for tungsten and steel both tend to level off for the larger thicknesses, probably because prompt (n, γ) radiation from the inspection material begins to have a significant effect on the film for the longer exposures needed to inspect larger thicknesses. This effect does tend to reduce contrast sensitivity somewhat. For example, contrast sensitivities on steel degraded from about 2 to 3 percent as the material thickness increased from 1 to 3 in.

The effect of the gamma radiation can be completely eliminated by using transfer techniques. Although in this case, a new limit on inspection thickness is imposed when the exposure time required is such that the activity of the metal foil used to detect the neutron image becomes saturated. For a 0.010-in.-thick dysprosium metal detecting foil transferred to Type AA X-ray film, tungsten can be inspected in thicknesses up to $2\frac{1}{2}$ in., steel up to 3 in., and natural uranium up to $3\frac{1}{2}$ in. These limits can be extended by increasing the neutron beam intensity beyond the 10^7 n/cm^2-sec used for these tests, by using a faster film or by increasing film development time over the 5 min used in this study.

The contrast sensitivity obtained in these tests has been generally on the order of 2 percent. In most cases, there is a significant improvement in the exposure time required for neutron radiographic inspection of these materials as compared with the times required by other radiographic methods. This is particularly true for the heavier metals in thicknesses of 1 in. or more. The high quality of inspection possible, coupled with the improvement in required exposure time, makes the use of neutron radiographic inspection of heavy metals attractive.

Technique curves for Masonite have also been completed in order to gain experience with hydrogenous material. The curves for this material tend to level off for thicknesses greater than 2 in., for both transfer and direct exposures, when the Juggernaut reactor neutron beam is used. The apparent explanation for these effects is that gamma radiation in the beam begins to account for significant film exposure for the direct-exposure method and that fast neutrons in the beam are moderated within larger object thicknesses and tend to activate the detecting foil. Both these effects would be expected to reduce the contrast which could be observed on radiographs of larger thicknesses of Masonite.

Both these effects can be eliminated by using a neutron beam containing a lower intensity of fast neutron and gamma radiation. This has been confirmed by tests using the monochromatic neutron beam at CP-5 reactor. Even with these effects eliminated, however, the contrast sensitivity obtained for radiographs of larger thicknesses of Masonite was relatively poor. For inspection of materials up to $\frac{1}{2}$ in., thickness changes of about 4 percent could be observed; for material $\frac{1}{2}$ to 1 in. thick, 10 percent thickness variations were observed; beyond 1 in., it was difficult to observe thickness variations less than 25 percent. The multiple scattering of the thermal-neutron beam within these larger masses of material probably accounts for this result. The use of neutron radiographic inspection of hydrogenous material, therefore, appears very limited for material thicknesses greater than 1 inch.

d. Alpha Spectrometry. Work on α spectrometry as a means of isotopic analysis has continued. The technique previously reported, in which uranium was deposited on film, has been given up. The resolution obtained using this technique was only good for the highest-energy α line of the source. Lower-energy lines were obscured by scattering from the low-atomic-number material in the film base. A conventional technique of plating uranium on platinum was used to produce sources of much better quality. A resolution of 26 kev full width at half maximum for 4.763-Mev α particles was observed with a source containing 20 mg/cm^2. Lower-energy α lines with intensities of 1/25 that of the highest energy line were easily resolved.

A plating cell with a rotating cathode is being constructed similar to one described by D. E. Hull, The Counting Method of Isotopic Analysis of Uranium, MDDC 387. The quantity of uranium deposited by this method can be determined to 0.1%.

This plating cell may be useful for preparing samples of irradiated uranium. The glycerin-pool technique previously tried was not suitable, as the sample did not remain fixed under vacuum.

C. Development of Viewing Systems

As part of the program to develop shielding and optical glasses with improved resistance to radiation-induced coloration and other effects, the properties of induced color centers in glass are being compared with those induced in alkali halide crystals. Preliminary results with thallium-doped aluminum borate glass indicate that some of the observed intrinsic absorption and emission, and radiation-induced absorption is similar to that observed in thallium-doped potassium chloride crystals (KCl:Tl).

The thallium was introduced as Tl_2O in the melt of an aluminum borate glass (1 Al_2O_3 : 4.5 B_2O_3 : 1 K_2O). The concentration of Tl_2O ranged from 0.0003 to 0.05 molar. The wavelength of the intrinsic absorption and emission bands due to the Tl and the postulated electronic transitions are summarized in Table VII along with those for KCl:Tl. The emission band occurs in glass when the sample is exposed to 215-mμ light. The intrinsic absorption in the 215-mμ region probably consists of a number of overlapping bands, since Beer's law is not followed and at the upper limits of the concentration range studied there is evidence of other bands. The thallium probably acts as a glass modifier, going into the glass as Tl^+. The change in absorption with concentration may be due to the thallium ions taking different positions in the glass structure.

Table VII. Wavelengths of Absorption and Emission Bands

	Tl-doped Aluminum Borate Glass	KCl:Tl	Transition
Absorption Bands	Below 200 mμ (Peak position unknown)	196 mμ	$6^1S_0 - 6^1P_1$
	-	205 mμ	-
	215 mμ	247 mμ	$6^1S_0 - 6^3P_1$
Emission Band	295 mμ	305 mμ	$6^3P_1 - 6^1S_0$

Preliminary measurements of optical absorption along with thermal and optical bleaching experiments have been carried out on gamma-irradiated samples. There is indication that some of the color centers present in irradiated KCl:Tl are also probably present in the irradiated thallium-doped aluminum borate glass.

D. Heat Engineering

1. EBWR Plutonium-recycle Core Studies

A study has been undertaken to determine the hydrodynamic behavior of the proposed plutonium-recycle core to be irradiated in the EBWR facility at a power level of 60 Mwt. The analysis is based on the use of the oxide-fueled, pin-type elements, for which the fuel pin has a diameter of 1.067 cm and an active fuel length of 122 cm. The elements will be arranged in subassemblies to form a core about 5 ft in diameter and 4 ft high. The core, however, will consist of three regions (a) a central plutonium-fueled zone; (b) a U^{235}-fueled driver zone; and (c) a natural-uranium buffer zone.

In order to calculate average steam void fractions accurately, it has been necessary to introduce an empirical modification in the RECHOP computer code based upon results from the recent EBWR experience. This will necessitate the use of at least two iterations before the second physics iteration, which uses the PDQ computer code to calculate the power distribution. The necessary modification is being effected and computations will be completed shortly.

2. Transient Behavior of Natural-circulation Loop Operating Near the Thermodynamic Critical Point

The purpose of this study was to investigate both analytically and experimentally the transient behavior of a natural-circulation loop in the near-critical region. In particular, attention was directed to the pressure and flow fluctuations which have been observed in previous studies. A natural-circulation loop using dichlorotetrafluorethane (Freon-114) as the circulating fluid was constructed and instrumented to measure and record pressure and flow fluctuations. The basic mechanism of flow and pressure fluctuations, from reports in the literature, appear to be independent of the system fluid. Freon-114 was selected as the system fluid because of the ease of handling and because of the low critical pressure and temperature (474.18 psia and 294.26°F).

The experimental portion of this work showed the conditions under which the transients occurred. The circulating system operated stably except in the thermodynamic region, which is identified as the maximum on the curve showing the product of density and enthalpy plotted versus temperature at a constant pressure.

Based upon the experimental results, analytical equations are being written to account for the transients in pressure and flow.

3. Sodium-expulsion Studies

The behavior of sodium coolant during fast power transients and its effect on reactor safety is being investigated. An idealized physical model for transient film boiling has been proposed which provides for the effects of variable wall temperature (in time). The variations of wall temperature to be considered are: (a) step-exponential rise; (b) step-sinusoidal rise; and (c) step rise. The mathematical formulation of the model resulted in a first-order, non-linear, partial differential equation. The equation was solved numerically on the PACE analog computer and compared with an analytical solution. Preliminary results indicate that the difference between numerical and analytical solutions for a simple step change in wall temperature is about 0.10%.

E. Chemical Separations

1. Chemical-Metallurgical Process Studies

a. Chemistry of Liquid Metals. The solubilities of barium, lanthanum, cerium, protactinium, and neodymium in zinc at 550°C are presented in Figure 7, as well as the solubilities in cadmium at 400°C of lanthanum, cerium, protactinium, neodymium, and samarium. In the cadmium systems, the equilibrium solid phases for all of the light rare earth metals were found to have the same type of structure (cubic $BaHg_{11}$). It was also found that the solubilities of the elements in cadmium increase in a smooth and regular fashion with increasing atomic number, presumably as a result of a uniform change in the free energy of formation of the intermetallic compounds and excess free energies of the solutes. The solubilities of the light rare earth metals in zinc do not increase in a regular manner, probably because the equilibrium solid phases have a variety of structures. The equilibrium solid phases found are $BaZn_{13}$ and $LaZn_{13}$ ($NaZn_{13}$ structural type), $CeZn_{11}$ and $PrZn_{11}$ ($BaCd_{11}$ structural type), and $NdZn_{12-x}$ (epsilon UZn_{12-x} structural type).

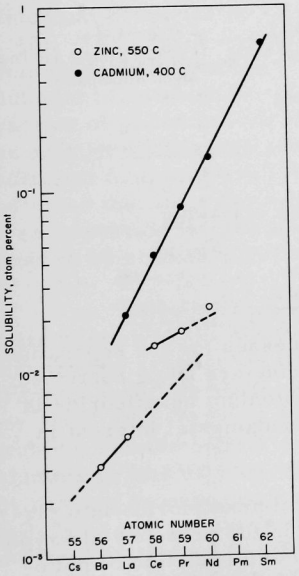

Figure 7. Solubilities in Zinc and Cadmium

Additional X-ray data are now available to supplement the effusion results previously obtained for the yttrium-zinc system (see

Progress Report for December 1962, ANL-6672, p. 33). The results of this study confirm the existence of the phases Y_2Zn_{17}, YZn_3, and YZn_2. Phases with the following stoichiometries seem probable: YZn_{12}, YZn_5, and $YZn_{4.5}$.

b. Reduction of Thorium Dioxide. In laboratory-scale work on the reduction of thorium dioxide to the metal by zinc-magnesium solutions, the flux used was composed of a mixture of fused halide salts containing only magnesium cation. The objective of this work was to determine the range of magnesium concentrations in the metal phase over which thorium may be completely reduced to form a product solution containing 9.1 w/o thorium. At 800°C, this range was found to be about 5 to 15 w/o magnesium (see Figure 8). Additional studies are being made in an effort to increase the thorium loadings in the system.

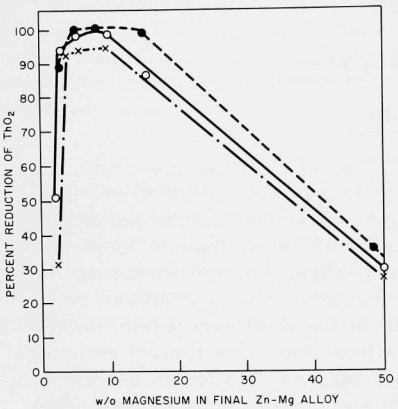

FLUX COMPOSITION

× 60 m/o $CaCl_2$, 30 m/o $MgCl_2$, 10 m/o CaF_2
○ 47.5 m/o $CaCl_2$, 47.5 m/o $MgCl_2$, 5 m/o CaF_2
● - 90 m/o $MgCl_2$, 10 m/o MgF_2

EXPERIMENTAL CONDITIONS

600 g MgZn Alloy
12.5 g Mg (React MgO)
300 g Flux
68.3 g ThO_2 Feed

800°C - 4 hr
850°C - Sample and Pour
Argon Atmosphere

Figure 8. Effect of Magnesium Concentration in Zinc on Reduction of Thorium Dioxide

2. Fluidization and Fluoride Volatility Separations

a. Fluoride Separations. Studies of processes for the separation of plutonium hexafluoride from uranium hexafluoride are being continued. The effect of radiation on the decomposition of plutonium hexafluoride is being studied to provide information which is of fundamental interest in the development of these processes.

The gamma decomposition of plutonium hexafluoride into plutonium tetrafluoride and fluorine when irradiated in the presence of krypton continues to be studied. Experiments on the gamma irradiation of plutonium hexafluoride samples (at 80 mm Hg pressure) containing krypton at

one-half atmosphere and one atmosphere have resulted in G values* of about 3.5 and 4.5, respectively. The total absorbed energy doses for the runs were about 3.5×10^{21} and 2.4×10^{21} ev, respectively. The G value of about 3.5 at one-half atmosphere confirms the previously reported G value of 2.9 for a similar experiment (see Progress Report for December 1962, ANL-6672, p. 34). The G value of 4.5 for the run made with krypton at one atmosphere is not in agreement with a previously reported G value of 6.4 for a similar experiment. Further experiments are planned to resolve this difference.

Additional data have been obtained on the alpha-induced decomposition of gaseous plutonium hexafluoride to plutonium tetrafluoride and fluorine (see Progress Report for October 1962, ANL-6635, p. 43). The decomposition rates of plutonium hexafluoride at 100 mm Hg pressure at room temperature were determined in six runs, each of about 176-day duration. Two runs were carried out in each of the following: nickel, Pyrex, and quartz spheres having volumes of about 127, 140, and 120 cc, respectively. In nickel vessels, the average decomposition rates were 0.25 and 0.21 percent per day; in Pyrex and quartz vessels, the decomposition rates were 0.34 and 0.23 percent per day.

Additional experimental work has been done to evaluate the filters employed in the ventilation systems of facilities used for handling plutonium hexafluoride (see Progress Report for June 1962, ANL-6580, p. 42). The filters are being evaluated for efficiency in removing plutonium particulate matter resulting from the vapor-phase hydrolysis of plutonium hexafluoride. Experimental results indicated that the smallest fraction of plutonium passed through two AEC-type filters in series when the amount of released plutonium hexafluoride was large and there was sufficient moisture available for complete hydrolysis. The results also indicated that the agglomeration of particles and the loading of the filters were important factors in the filter performance. The particles were found to be smooth spheres with a mean diameter of about 0.017 μ.

b. Direct Fluorination of Uranium Dioxide Fuel. Engineering-scale studies have continued on the development of a two-zone oxidation-fluorination scheme for the conversion of uranium dioxide pellets into uranium hexafluoride in a single reactor (see Progress Report for November 1962, ANL-6658, p. 51). In this scheme, the lower zone consists of uranium dioxide pellets and the upper zone consists of alumina grains. Alumina grains also fill the voids in the lower uranium dioxide pellet bed. By passing an oxygen-nitrogen mixture through the lower reaction zone, U_3O_8 fines are produced. These fines are elutriated from the pellet bed, and are fluorinated in the upper reaction zone. The transport of uranium oxide (U_3O_8) fines from the uranium dioxide pellet bed to the fluorination

*Molecules decomposed per 100 ev of radiation.

zone is facilitated by the presence of the fluidized alumina. By imposing a temperature gradient through the pellet bed, the oxidation of the uranium dioxide occurs near the top of the bed. This portion of the bed is maintained at a temperature of about 400°C. A lower temperature is maintained in the lower portion of the pellet bed; thereby, the oxidation reaction of the uranium dioxide pellets in this portion of the bed is minimized.

Two runs have been made with a 12-in.-deep pellet bed and a 24-in.-deep fluidized alumina zone above the pellet bed. One run was stopped for a time when a plug developed in the fluorine inlet line after 2.5 hr of operation and was terminated when caking occurred in the pellet bed after 5 additional hours of operation following the replacement of the fluorine inlet line. The other run was made to investigate gas pulsing in the lower zone to improve transport of fines through the pellet bed to the upper zone and thereby reduce the tendency toward caking in the bed. The pulse was directed upward toward the pellet bed by providing an injection tube beneath the pellet-bed support. The gas pulsing in the pellet bed resulted in a rapid production and transport of the oxide fines, but the pulsing conditions used in this run produced excessive elutriation and deposition of the oxide fines above the alumina bed. Moreover, the temperature gradient in the pellet bed was disrupted by the pulsing, and a satisfactory temperature gradient could not be re-established in the pellet bed. An improved method of controlling the gas pulse will be used in further studies of this process.

c. Decladding of Fuel Elements by Fluid-bed Oxidation. Preliminary experiments were carried out in an effort to extend fluid-bed oxidation to the separation of uranium dioxide pellets from stainless steel cladding in typical fuel elements. This method involves the oxidation with air of the uranium dioxide pellets to a higher oxide (U_3O_8). The difference in the densities of the two oxides (UO_2 and U_3O_8) causes large internal stresses which fragmentize the uranium dioxide pellets. The uranium oxide (U_3O_8) fines produced in the oxidation zone of the two-zone oxidation-fluorination reactor will be elutriated to the fluid-bed fluorination zone. The cladding is not expected to react and will be removed mechanically from the reactor.

In the preliminary experiments, 40 one-in. lengths of simulated fuel elements were used as a randomly packed bed. The simulated fuel elements were made by placing two $\frac{1}{2}$-in.-diameter pellets of uranium dioxide in each of the close-fitting, one-in.-long stainless steel tubes. These tubes were open at both ends. A 2-in.-diameter nickel reactor was used. The results of a run made with an 8-in.-deep bed charge of uranium dioxide pellets and alumina grain showed that about one-half of the uranium dioxide was removed from the pellets in 5 hr at 400°C with air at a superficial gas velocity of 0.7 ft/sec.

d. Separation of Uranium from Zirconium by Chlorination and Fluorination. The development of a chlorination-fluorination scheme for reprocessing highly enriched uranium-zirconium alloy fuels was continued. In a recently reported run, the effect of multiple feed batching of alloy chips during the hydrochlorination step was investigated (see Progress Report for December 1962, ANL-6672, p. 36). Each charge consisted of 240 g of 5 w/o uranium-zirconium chips ($\frac{1}{8}$ to $\frac{1}{4}$ in. in size). The processing scheme involved the hydrochlorinations of three successive batches of alloy chips followed by a single fluorination step to recover the uranium from the Alundum in the fluid bed and in the off-gas filter beds. Data on the rates of hydrochlorination of the alloy chips have been previously presented (ANL-6672).

Information on the retention of uranium by Alundum was obtained from the analysis of samples of Alundum taken at half-hour intervals from the fluidized bed during the fluorination period (2 hr at 350°C and 6 hr at 500°C). The uranium content of the Alundum in the fluid bed was reduced from an initial value of 1.04 w/o to 0.13 w/o during the low-temperature fluorination period; further reduction in uranium content of the Alundum bed to 0.05 w/o was achieved during the first hour of fluorination at the higher temperature, but no additional removal of uranium was obtained during the remainder of the fluorination period. A final uranium content in the bed of 0.05 w/o corresponds to 0.4 w/o of the total initial uranium charge.

Thermal conductivity cells were used for continuous analysis of the hydrochlorination and fluorination reaction off-gas streams. Preliminary data indicated that about 90 percent of the uranium in the fluid bed and filter bed was recovered during the first 30 min of the low-temperature fluorination period.

A method is being developed for charging uranium-zirconium alloy fuel assemblies into a fluid-bed reactor when the bed is in a static condition. This technique will be helpful in pilot-plant and plant-scale operations. The method involves the introduction of intermittent pulses of gas to the bottom of the reactor after the fuel element has been loaded onto the top surface of the static bed. The pulses result in an alternate expansion and settling of the bed. The element drops while the bed is momentarily expanded. The pulsing action is controlled so that the element is lowered slowly into the bed. The possibility of damage to the bottom of the column as a result of an element falling rapidly through the column is eliminated by this technique.

Preliminary data indicate that the pulsing technique is a satisfactory method for lowering a multiplate-type fuel element into the primary fluid bed reactor. Further experimentation is planned to determine quantitatively the effects of system variables on the settling rate

of multiplate fuel elements in a pulsed bed of solids. The system variables to be studied will include the size and duration of the pulse, the effect of the cross-sectional configuration of the element, bed particle size, and the effect of superimposing the pulses on a continuous (sub-fluidizing) flow of gas in the fluid-bed column.

3. Calorimetry

Two series of combustions of zinc in fluorine have been completed. Preliminary calculations indicate that the energy evolved per gram of zinc burned is approximately 2788 cal.

Calorimetric combustions of niobium in fluorine are in progress. Exploratory combustions of silicon carbide in fluorine are beginning.

IV. ADVANCED SYSTEMS RESEARCH AND DEVELOPMENT

A. Argonne Advanced Research Reactor (AARR)

1. General Program

The general research and development program for the AARR project to be performed during the balance of FY 1963 and in FY 1964 is as follows:

During the remainder of FY 1963, the critical experiment safety analysis report will be completed and submitted for approval, cell modification work will continue, and the fuel will be ordered. In addition, hydraulics testing of sample fuel assemblies will be performed in an existing test facility. A study will be made of the requirements for a heat transfer loop to be constructed in the following year. The critical experimental program will be performed in FY 1964. In addition, studies on the preliminary design of the building layout and containment, coolant systems, reactor vessel, core components, and experimental facilities will proceed and permit completion of both the preliminary AARR Safety Analysis Report and a design prospectus.

2. Core Physics

When a control rod is partially inserted in the core, the power in neighboring fuel plates is depressed opposite the active portion of the control rod and elevated opposite the inactive, or follower, portion of the rod. Hot channels next to control rods have been examined in a series of three-dimensional calculations of neutron flux and power, followed by heat-removal calculations in which the axial heat distributions were well represented. The average heat flux was found to be 81% of the unrodded heat flux; the maximum heat flux was estimated to be 2.25 times this, however. The effect is to increase the overall maximum-to-average power generation by 36%. This problem may be alleviated by local flux suppressors, plate orientation, or fuel depletion, as well as by a variety of other means.

3. AARR Preliminary Safety Analysis

In the event of a radioactive release to the air within the reactor building, contaminated air will disperse through filters and then out of the stack and via building leakage. In the absence of stack ventilation, the building leak rate must be small enough to prevent hazard to the population at large. A detailed calculation was made as based on 100% core meltdown and a severe inversion outside. Meteorological data show that, even with a leak rate as high as 1% of the building volume for 24 hr, the exclusion area is well within ANL site boundaries, whereas the low population zone extends to the boundary of the town of Lemont, a few miles distant and the nearest population center.

B. Underseas Application of Nuclear Power

A study of the application of nuclear power to a small, manned oceanographic research submarine has been completed. The mission of the research submarine is twofold: (1) to investigate the migratory habits of the tuna, and (2) to explore the mineral resources on and below the ocean floor. To accomplish the first mission the vessel must be capable of 20 knots (submerged) for 24 hr, and for the second mission, must descend to 600 ft and provide power to equipment (for drilling, etc.) for a period of several days. The following design requirements are placed on the power plant:

(1) Compactness - must fit in a hull with a 15-ft-maximum-diameter and must occupy only one-fourth to one-third of the volume of a 100-ft-long vessel.

(2) Power - must provide 2000 shp for a period of one year before replacement.

(3) Schedule - must be capable of being built within one to two years by present technology.

The conclusion of this study is that a nuclear power plant with a highly-enriched, pressurized water reactor is capable of meeting the above requirements and is superior to other power sources (such as batteries, and fuel cells). A summary of the reactor design data is given in Table VIII.

Table VIII. Summary of Design Data

Overall Plant Data	
Thermal Power	7.75 Mw
Output	2000 shp or 1500 shp + 350 kwe
Overall Efficiency	19.0%
Power Density	225 kw/liter
Components	
Core Design	
Dimensions	13.95 in. in dia x 13.8 in. high
Volume	1.22 ft^3 = 34.5 liters
Fuel Material	93.5% enriched UO_2 + stainless steel
U^{235} Content	27.27 kg
UO_2 Content	33.13 kg
Composition of Fuel	
UO_2	47.2%
Stainless Steel	52.8%
Fuel-element Design	20-mil plate of UO_2 + stainless steel with 5-mil stainless steel clad; 51.8-mil coolant channel

Table VIII (Contd.)

Metal-to-water Ratio	0.64
Reflector, Water	8.66 in.
Thermal Shield, Steel	2 in.
Pressure Vessel	
Dimensions	3.0-ft dia x 5.0 ft high
Thickness	1.75 in.
Shielding, Vessel	
Dimensions	9-ft dia x 10 ft high
Thermal Design	
Coolant	H_2O
Pressure	1200 psia
Temperature	
Inlet	452°F
Outlet	472.5°F
Flow Rate	2910 gpm; 1.2×10^6 lb/hr
Steam Generator	
Dimensions	4-ft dia x 9.5 ft long
Steam	
Pressure	200 psia
Temperature	382°F
Rate	23,500 lb/hr
Pressurizer, Dimensions	3.3-ft dia x 4.6 ft high
Main Primary Pump	
Flow	2910 gpm
Head, water	20 ft
Pump Power	13 hp
Turbine	
Power	1500 kw; 2000 shp
Steam	
Inlet	195 psia; 382°F
Outlet	3.5 psia; 145°F, 14% moisture content
Dimensions	~ 8-ft dia x 9 ft long
Condenser	
Dimensions	2.5-ft dia x 9.5 ft long
Heat Removal Rate	2.1×10^7 Btu/hr
Main Secondary Pump	
Flow	60 gpm
Head, water	425 ft
Pump Power	6.5 hp
Total Volume of All Components	~ 1500 ft^3

The 10-ft-high, 9-ft-diameter right cylinder reactor complex will fit in the submarine vessel and also allow for a personnel passage. Although it is not claimed that the power plant design is optimized for this type of reactor, a substantial reduction in size does not seem likely. A 15-ft-diameter submarine, therefore, is close to the minimum size that could carry this type of nuclear power plant.

C. Rocket Fuel Test Reactor (RFTR)

As part of a program to study and evaluate the application of nuclear reactors for thermal-rocket propulsion, the concept of using a reactor to test fractions of prototype cores under design conditions is being investigated. A test reactor should, therefore, in principle, consist of a center test section surrounded by a peripheral driver section. The test reactor concept should reduce testing costs, including the reduction in quantities of hydrogen required for tests of long duration.

The minimum power density for some proposed rocket reactor cores is 10 Mw/liter. It is desired to test a fraction of the prototype core with a volume as large as 20 liters. The driver should be loaded such that the power density ratio between the test section and driver is 10 to 1 or better. At the same time the total power of the driver should not exceed several hundred megawatts.

The study will consider the feasibility of designing an all-purpose reactor, namely, one that will test both the fast, epithermal, and thermal fuel elements. Based on the current analysis it appears that any such system will have to operate by adjusting the spectrum in the driver by inserting or removing moderator in a prescribed manner to match the spectrum desired in the test region to avoid severe flux peaking in the system.

Preliminary physics calculations for a number of design concepts have been made with use of the RE-122 code and cross section set 201. One concept investigated was a very lightly loaded, graphite-moderated thermal driver. Another concept studied was a driver reactor similar in composition to the FFTR (Fast Fuel Test Reactor).[7] This system has an epithermal spectrum and the flux depression in the test section is much less severe than in the graphite thermal driver. Some results of these preliminary calculations are shown in Table IX.

---

[7] R. Brubaker, H. H. Hummel, J. H. Kittel, A. McArthy, and A. Smaardyk, Fast Fuel Test Reactor - FFTR Conceptual Design Study, ANL-6194 (Aug 1960).

Table IX. RE-122 Calculations* for Two Rocket Test Driver Concepts

Prob. No.	Test Section Volume (ℓ)	Driver				Ratio of Power Densities		Driver Power Required (Mw)
		Fuel	Moderator	Ratio of Moderator to Fuel	Coolant	Center of Test Region / Max in the Driver Region	Center of Test Region / Edge of Test Region	
100	5	U^{235}	Graphite	50,000	Air	35	12	~1000
102	20	UO_2	Beryllium	30	Sodium	5	1.06	~150

*Spherical Geometry

As shown, the center-to-edge power ratio is reduced from 12 to 1.06 in going from a well-thermalized to an epithermal spectrum. The test section-to-driver power density ratio, however, is only 5 for the FFTR driver (Prob. 102). This means that a power density of ~2 Mw/liter (max) is required for this driver. Additional studies are in progress.

V. NUCLEAR SAFETY

A. Thermal Reactor Safety Studies

1. Metal Oxidation and Ignition Studies

The rates of oxidation of uranium by air at temperatures of 700°C and above are being studied to determine the nature of the oxide coating produced at these temperatures and to evaluate the degree of protection that the coating affords against further oxidation of the uranium. It is also planned to assess the role of nitrogen in the oxidation reaction.

In a first series of reactions, a mixture of air and argon was passed over one-cm cubes of uranium heated to 700°C. X-ray diffraction studies indicated that the only oxide formed was U_3O_8. The oxide was granular and, although much of the oxide dropped off the samples, a relatively thick coat remained on the samples throughout the run. The rate data obtained during the course of this series are being evaluated.

Isothermal oxidation studies of plutonium were continued. Between 140 and 300°C, the oxidation reaction is best described by postulating a parabolic rate law in the initial stage of the reaction, followed by a linear rate law. Between 140 and 200°C, the para-linear rate is followed by a much faster linear rate which does not appear to be temperature dependent. Only cubic plutonium dioxide was found in X-ray powder-diffraction studies of the oxide removed from the surface of the plutonium specimens.

2. Metal-Water Studies

Two new methods of heating samples for metal-water reaction studies are being investigated. The first method depends upon the use of an induction-coupled argon plasma. The high temperatures (15,000°C) which can be attained in a plasma should make it possible to heat small particles to high temperatures in an inert atmosphere. The extent of reaction occurring upon dropping the heated material into water could be measured by established procedures, e.g., by measuring the amount of hydrogen evolved. Investigation of the plasma method has been halted in order to evaluate a second heating method, namely, the use of an intense beam from a high-energy laser. This latter method offers the possibility of heating small samples extremely rapidly to very high temperatures in a water environment. Tests made elsewhere on large samples have shown that good control of power input to the sample can readily be attained.

In-pile studies of metal-water reactions in TREAT are continuing. Metallographic examinations of residues from a series of runs with 2S aluminum-clad, 77 weight percent aluminum-23 weight percent uranium core plates were completed. Some striking differences in the appearance of the fuel samples were observed. The nature of the residues appeared to

be dependent upon the reactor energy to which the samples were subjected. The original core material had three phases - probably UAl_4 and UAl_3 dispersed in an aluminum matrix. Samples subjected to energies below 430 cal/g showed no separate phases, but appeared instead to be a porous agglomeration of small rounded crystals. Energies between 430 cal/g and 770 cal/g resulted in residues in which large slab-like crystals were randomly scattered in a matrix of many phases. Energies above 770 cal/g resulted in a material which appeared to be a eutectic in which small phase fields were finely dispersed. At the higher energies (above 430 cal/g), the extent of the metal-water reaction was appreciable (above 10 percent) and both uranium oxide and aluminum oxide were found to be present.

B. Fast Reactor Safety Studies

1. Meltdown Experiments

TREAT is being used to perform in-pile experiments to study the causes and characteristics of failure of fast-reactor fuel elements, and to survey the mechanisms influencing the movement of fuel.

a. Summary of Tests on Fast-reactor-type Oxide Samples. The work performed to date in the meltdown experiments with EBR-II-sized uranium oxide reactor fuel samples in TREAT is reported. The manner of fuel failure and motion characteristics under conditions of transient heating in the absence of sodium were observed. Inert gas rather than sodium was selected for the experimental environment to permit high-speed photography of the samples during the tests, to eliminate destructive thermal stresses in the clad or oxide pellets due to sharp thermal gradients which would result from the presence of liquid metal coolant, and to allow the use of fast-response thermocouples for the measurement of transient temperatures on the cladding.

Cladding materials used were stainless steel, niobium, and tantalum. In the tests, samples were exposed to transient power bursts of the order of 0.5-sec duration, with rates of temperature rise up to the order of 5000°C/sec. Temperature rise in the fuel during the power burst were estimated to be comparatively uniform as a function of radius. Cladding temperature lagged behind the fuel temperature, thermal equilibrium between fuel and clad being reached about 2 sec after the power peak.

Steel-clad elements were found to fail in a comparatively nonviolent fashion near the melting point of steel, due to internal pressure buildup (estimated to be about 5 atm) of the inert gas bond in the element. When heated beyond the failure threshold, the steel-clad specimens collapsed under the influence of gravity. A maximum cladding temperature of about 1600°C marked the threshold at which a layer of loose bonded oxide appeared in the central region of the solid oxide fuel cylinders. Exposures at higher temperature tended to cause the oxide cylinders to

break into shorter axial lengths. The high-temperature failure of a tantalum-clad element (maximum recorded cladding temperature of about 2400°C) was accompanied by extensive movement of fuel from the sample, and resulted in production of small fragments.

Oxide cylinders did not exhibit the familiar pattern of radial and circumferential cracks displayed by fuel subjected to steady-state exposure. However, this can be attributed to a difference in oxide thermal stresses between those arising from typical steady-state radial temperature distributions and the transient radial temperature distributions calculated for these specimens. The tests showed that, generally, failure of this type of element under these conditions of transient heating is not violent. Gross disintegration of the structure occurs by melting.

b. Small (Package) Sodium Loop. A low-power measurement was made in the TREAT reactor with an empty prototype package loop in the central test hole. The loop is designed to fit within the space of a TREAT fuel element. The worth of the loop was reported to be -3.4% Δk with respect to a void in the central test hole position. This result implies a worth of -3.95% Δk for a dummy element in this position and is in reasonable agreement with a value of -4.3 Δk which was previously calculated by two-dimensional diffusion theory.

A power calibration value of 8.77×10^{10} fissions/gm of sample fuel per megawatt-second was obtained for an exposure of a 4.1% enriched EBR-II element in the loop. The determination was made by radiochemical analysis of the sample element and enriched foils. This value is approximately two-thirds of the calibration factor for the same sample in the stagnant sodium capsule.

The handling and shipping cask for the loop has been received from the subcontractor, and found to be acceptable from the standpoint of shielding based on tests with a radioactive source.

c. Installation of Large Sodium Loop in TREAT. The three immersion heater assemblies for the sodium-loop storage tank passed helium leak tests. The insulation resistance of the heaters was also found to be satisfactory after cycling thermally to 500°C in NaK. The second resistance-type sodium-tank-level probe was operating properly in a NaK-filled autoclave at the end of the month.

Installation of conduit between the control panels on the main floor of the reactor building and the sodium equipment room is in progress.

A contract was awarded for installation of air cooling and ventilation systems for the sodium equipment room.

VI. PUBLICATIONS

Papers

GAMMA RAY DISCRIMINATION IN A PROTON RECOIL PROPORTIONAL COUNTER

E. F. Bennett

IAEA Symposium on Neutron Detection, Dosimetry, and Standardization, Harwell, England, December 10-14, 1962. Abstract No. SM-36/62.

FAST NEUTRON DOSIMETRY FOR RADIATION DAMAGE STUDIES

A. D. Rossin and R. J. Armani

IAEA Symposium on Neutron Detection, Dosimetry, and Standardization, Harwell, England, December 10-14, 1962. Abstract No. SM-36/86.

OPTIMIZATION OF EFFICIENCY OF A CESIUM-DIODE CONVERTER

C. K. Sanathanan

J. Appl. Phys. 33, 3491-3493 (December, 1962).

REAL ROOTS OF THE EQUATION $x \tan y + \tanh y = 0$ (Review)

Henry C. Thacher, Jr.

Mathematics of Computation, Vol. 17, No. 81, p. 90 (January, 1963). Abstract.

INELASTIC SCATTERING OF FAST NEUTRONS FROM Cu, Zr, and Nb

D. Reitmann and A. B. Smith

Bull. Am. Phys. Soc. 8, 81 (1963). Abstract.

OPTICAL MODEL FOR LOW-ENERGY NEUTRONS

P. A. Moldauer

Bull. Am. Phys. Soc. 8, 81 (1963). Abstract.

USING PLUTONIUM IN FAST REACTORS

Harry H. Hummel, Milton Levenson, Leonard E. Link, Robert E. Machery, and Wallace R. Simmons

Nucleonics 21, (1) 43-47 (January, 1963).

SOME NEW TECHNIQUES OF NUMERICAL ANALYSIS

Henry C. Thacher, Jr.

Proceedings of the 5th Annual Meeting of POOL, Philadelphia, Pa., April 2-4, 1962, Assoc. of Users of General Precision Electronic Computers, Burbank, Cal., 1962. pp. 72-86.

OPTICAL PROPERTIES OF IRRADIATED THALLIUM DOPED KCl AND ALUMINUM BORATE GLASS

A. K. Ghosh, C. J. Delbecq and P. H. Yuster

Bull. Am. Phys. Soc. 7, 616 (December, 1962).

PENETRATION RATE STUDIES OF STAINLESS STEEL BY MOLTEN URANIUM AND URANIUM-FISSIUM ALLOY
C. M. Walter and L. R. Kelman
J. Nuc. Matls. 6 (3) 281-290.

URANIUM DIOXIDE: PROPERTIES AND NUCLEAR APPLICATIONS
J. H. Handwerk, Book Review
J. Am. Cer. Soc. 45 (4) 106-107.

The following papers were presented at a symposium, Current Trends in Nuclear Power, sponsored by the University of Arizona in cooperation with Argonne National Laboratory, at Tucson, Arizona, February 26-March 2, 1962, and appear in the Proceedings:

WASTE DISPOSAL
A. A. Jonke
pp. 100-106

FUEL REPROCESSING
Stephen Lawroski
p. 44 Abstract

METALLIC FUELS
F. G. Foote
pp. 19-25

PLUTONIUM TECHNOLOGY
F. G. Foote
pp. 93-99

CURRENT TRENDS IN REACTOR SAFETY
R. O. Brittan
pp. 107-113

RESEARCH REACTORS
C. N. Kelber
pp. 14-18

FAST REACTORS
L. J. Koch
p. 88 Abstract

STATUS OF BOILING WATER REACTOR TECHNOLOGY ENGINEERING DESIGN
C. V. Pearson
pp. 30-43

ADVANCED REACTOR CONCEPTS AND A LOOK AHEAD
B. I. Spinrad
pp. 121-126

ANL Reports

ANL-6532 SWELLING OF URANIUM AND URANIUM ALLOYS ON POSTIRRADIATION ANNEALING
B. A. Loomis and D. W. Pracht

ANL-6616 DESIGN SUMMARY REPORT ON THE JUGGERNAUT REACTOR
J. R. Folkrod, G. Ember, W. Kolb, J. Saluja, and D. P. Moon

ANL-6642 THE NITRIDATION RATES OF URANIUM-FISSIUM ALLOYS
J. P. LaPlante and R. K. Steunenberg

ANL-6645 ANALOG COMPUTATION OF TEMPERATURE DISTRIBUTION IN SOLIDS WITH ELECTRICAL HEAT-GENERATION AND TEMPERATURE-DEPENDENT PROPERTIES
Darrel G. Harden and Lawrence T. Bryant